Molecular Biology of the Cell
Vol. 8, 1273–1291, July 1997

A Novel a-Factor-related Peptide of *Saccharomyces cerevisiae* that Exits the Cell by a Ste6p-independent Mechanism

Peng Chen,* Jonathan D. Choi,* Rong Wang,† Robert J. Cotter,† and S. Michaelis*‡

*Department of Cell Biology and Anatomy and †Department of Pharmacology and Molecular Sciences, The Johns Hopkins School of Medicine, Baltimore, Maryland 21205

Submitted February 6, 1997; Accepted April 17, 1997
Monitoring Editor: Randy Schekman

Many secreted signaling molecules are synthesized as precursors that undergo multiple maturation steps to generate their mature forms. The *Saccharomyces cerevisiae* mating pheromone **a**-factor is a C-terminally isoprenylated and carboxylmethylated dodecapeptide that is initially synthesized as a larger precursor containing 36 or 38 amino acids. We have previously shown that the maturation of **a**-factor occurs by an ordered biogenesis pathway involving 1) three C-terminal modification steps, 2) two N-terminal proteolytic processing events, and 3) a nonclassical export mechanism mediated by the ATP-binding-cassette (ABC) transporter Ste6p. In the present study, we demonstrate that an unexpected and abundant **a**-factor-related peptide (AFRP) exists in the culture fluid of *MAT***a** cells and that its biogenesis is integrally related to that of mature **a**-factor itself. We show by purification followed by mass spectrometry that AFRP corresponds to the C-terminal 7 amino acids (VFWDPAC) of mature **a**-factor (YIIKGVFWDPAC), including both the farnesyl- and carboxylmethylcysteine modifications. The formation and export of AFRP displays three striking features. First, we show that AFRP is produced intracellularly and that mutants (*ste24* and *axl1*) that cannot produce mature **a**-factor due to an N-terminal processing defect are nevertheless normal for AFRP production. Thus, AFRP is not derived from mature **a**-factor but, instead, from the P1 form of the **a**-factor precursor. Second, fusion constructs with foreign amino acids substituted for authentic **a**-factor residues still yield AFRP-sized molecules; however, the composition of these corresponds to the altered residues instead of to AFRP residues. Thus, AFRP may be generated by a sequence-independent but length-specific proteolytic activity. Third, **a**-factor and AFRP use distinct cellular machinery for their secretion. Whereas **a**-factor export is Ste6p-dependent, AFRP is secreted normally even in a *ste6* deletion mutant. Thus, AFRP may exit the cell by another ATP-binding-cassette transporter, a different type of transporter altogether, or possibly by diffusion. Taken together, these studies indicate that the biogenesis of AFRP involves novel mechanisms and machinery, distinct from those used to generate mature **a**-factor. Because AFRP neither stimulates nor inhibits mating or **a**-factor halo activity, its function remains an intriguing question.

INTRODUCTION

Extracellular signaling molecules are often synthesized as precursors that undergo complex modification and

‡ Corresponding author: Department of Cell Biology and Anatomy, The Johns Hopkins School of Medicine, 725 North Wolfe Street, Baltimore, MD 21205.

proteolytic processing events during their biogenesis (Resnick and Zasloff, 1992). The precise characterization of the site of these processing reactions within the maturing molecule is critical for providing insight into the biochemical nature of these reactions and ultimately for identifying the cellular components that mediate them.

The yeast mating pheromone **a**-factor is an isoprenylated and carboxylmethylated oligopeptide signaling molecule, initially synthesized as a larger precursor. The biogenesis of the **a**-factor precursor to yield mature bioactive **a**-factor is a multistep process that involves C-terminal modification, N-terminal processing, and secretion via a nonclassical export mechanism (Chen *et al.*, 1997; see also Figure 13 for a summary of the **a**-factor biogenesis pathway). The C-terminal modification of the **a**-factor precursor is directed by its C-terminal CAAX motif (C is cysteine, A is an aliphatic residue, and X is one of many residues), which is present in all proteins that are destined for isoprenylation (Zhang and Casey, 1996). The C-terminal modification of the **a**-factor precursor, as well as of Ras and other CAAX proteins, has three ordered steps: covalent addition of a farnesyl isoprenoid by the Ram1p/Ram2p prenyltransferase, proteolytic removal of the three terminal AAX residues (which correspond to VIA for **a**-factor), by Rce1p and possibly Afc1/Ste24p and methylation of the newly exposed cysteine carboxyl group by the Ste14p methyltransferase (see Figure 13; He *et al.*, 1991; Hrycyna *et al.*, 1991; Ashby *et al.*, 1992; Hrycyna and Clarke, 1992; Boyartchuk *et al.*, 1997). The N-terminal proteolytic maturation of **a**-factor, which takes place after the completion of C-terminal modification, involves two sequential proteolytic cleavage events. The first cleavage occurs within the N-terminal extension (between T7 and A8 of the **a**-factor precursor); the second cleavage occurs at the junction of the N-terminal extension and mature **a**-factor (between N21 and Y22) to generate mature bioactive **a**-factor (Chen *et al.*, 1997; see also Figure 13). These cleavages are mediated by the zinc metalloproteases Ste24p and Axl1p, respectively (Adames *et al.*, 1995; Fujimura-Kamada *et al*, 1997). Once formed, mature **a**-factor is exported from the cell. An intriguing feature of the biogenesis of **a**-factor is its nonclassical export mechanism. Unlike most secreted molecules that are matured and exported through the classical secretory pathway (Schekman, 1985; Pryer *et al.*, 1992), the export of **a**-factor is mediated by Ste6p, which belongs to the ATP binding cassette (ABC) superfamily of transporters (Kuchler *et al.*, 1989; Michaelis, 1993).

Our understanding of **a**-factor biogenesis, described above, is based upon our characterization of the **a**-factor biosynthetic intermediates P0, P1, P2, and M (see Figure 13). These intermediates can be detected by metabolic labeling, immunoprecipitation, and SDS-PAGE analysis of **a**-factor, expressed from either of two functionally redundant genes, *MFA1* or *MFA2* (Brake *et al.*, 1985; Michaelis and Herskowitz, 1988). We have established the identity of these species by determining their N-terminal amino acid composition and C-terminal modification status. P0 corresponds to the unmodified **a**-factor precursor, P1 corresponds to the fully C-terminally modified precursor, P2 corresponds to the first N-terminally cleaved species, and M corresponds to mature **a**-factor (Chen *et al.*, 1997).

During our initial analyses of **a**-factor biogenesis, we occasionally observed a novel **a**-factor-related peptide (hereafter referred to by the acronym AFRP) whose origin was puzzling. The AFRP species could often, but not always, be observed in intracellular immunoprecipitates, depending upon the preparation of **a**-factor antiserum that we used (see for instance Sapperstein *et al.*, 1994; Chen *et al.*, 1997). On the other hand, AFRP was always apparent along with mature **a**-factor upon examination of the extracellular culture fluid, when this fraction was examined in the absence of immunoprecipitation. These findings suggested that AFRP is recognized by **a**-factor antiserum, but very poorly.

AFRP is the focus of the present study. AFRP is abundant; it is present at approximately the same level as mature **a**-factor itself. We demonstrate that AFRP, like **a**-factor, is derived from the *MFA1* and *MFA2* genes and that AFRP is an "alternative cleavage product" generated in parallel with mature **a**-factor. By plasma desorption mass spectrometry (PDMS) of high-pressure liquid chromatography (HPLC)-purified AFRP, we show that AFRP corresponds to the C-terminal seven residues of mature **a**-factor, including its farnesyl and carboxylmethyl modifications. AFRP also contains an additional 16 mass units, most likely due to the addition of an oxygen on the side chain of one of its residues. We find neither **a**-factor-like activity nor inhibitory activity associated with the HPLC fraction containing AFRP, so that even though AFRP is abundant its biological role is not clear. In addition to determining its composition, we have examined the biogenesis of AFRP. These studies reveal three striking aspects of the processing and export of AFRP. First, AFRP is generated from a precursor form of **a**-factor, P1, in parallel with, and not from, mature **a**-factor. Second, our data suggest that AFRP could be generated by a sequence-independent but length-measuring proteolytic activity that may use prenylcysteine as its landmark and cleave a relatively fixed distance from it, regardless of the amino acids located at that site. Third, unlike mature **a**-factor, the export of AFRP is *STE6* independent, suggesting that AFRP may use a novel transporter for its exit from the cell. Thus, these results suggest the existence of novel proteolytic processing and export components specifically dedicated

Table 1. *S. cerevisiae* strains used in this study

Strain	Genotype	Source
SM1058	*MAT***a** *trp1 leu2 ura3 his4 can1*	Michaelis and Herskowitz (1988)
SM1086	*MATα met1 his6 can1 cyh2 sst2-1*	Michaelis and Herskowitz (1988)
SM1188	*MAT***a** *ste14-Δ1::TRP1 trp1 leu2 ura3 his4 can1*	Hrycyna *et al.* (1991)
SM1229	*MAT***a** *mfa1-Δ1::LEU2 mfa2-Δ1::URA3 trp1 leu2 ura3 his4 can1*	Michaelis and Herskowitz (1988)
SM1458	*MAT***a** *mfa1-Δ1::LEU2 mfa2-Δ2::lacZ trp1 leu2 ura3 his4 can1*	Chen *et al.* (1997)
SM1646	*MAT***a** *ste6-Δ2::URA3 trp1 leu2 ura3 his4 can1*	Berkower and Michaelis (1991)
SM1863	*MAT***a** *ram2-1 leu2 ura3 his3 trp1 ade8 can1*	He *et al.* (1991)
SM1866	*MAT***a** *ram1-Δ1::URA3 trp1 leu2 ura3 his4 can1*	He *et al.* (1991)
SM3103	*MAT***a** *ste24-Δ1::LEU2 trp1 leu2 ura3 his4 can1*	Fujimura-Kamada *et al.* (1997)
SM3256	*MAT***a** *axl1::LEU2 ste23::LEU2 trp1 leu2 ura3 his4 can1*	Adames *et al.* (1995)

to the production of AFRP and distinct from those components known to mediate the biogenesis of **a**-factor.

MATERIALS AND METHODS

Yeast Strains and Media

Yeast strains used in this study are listed in Table 1. Complete medium (YEPD), synthetic drop-out medium (SC-URA and SC-TRP), and SD minimal medium were prepared as described previously (Michaelis and Herskowitz, 1988), except that drop-out medium is lacking L-methionine and L-cysteine for the metabolic labeling experiments with [^{35}S]cysteine. Where necessary, SD medium was supplemented with L-histidine (20 μg/ml), L-tryptophan (20 μg/ml), or L-leucine (30 μg/ml) and uracil (20 μg/ml). Strains were grown at 30°C, unless otherwise specified.

Plasmids and Manipulations of DNA

Plasmids used in this study are listed in Table 2. Mutant allele designations are also described in Table 2. Constructions were carried out as follows: The mutants *mfa1*::DP(21) and *mfa1*::DP(32) contain an insertion of two codons, DP, encoding a *Bam*HI recognition sequence just preceding codons 21 and 32 of *MFA1*, respectively. They were generated via site-directed mutagenesis (Kunkel *et al.*, 1987) using the oligonucleotide sequences oSM23 (5′-TTGATAATATAGGGATCCTTGTCCTTCTTT-3′) and oSM18 (5′-GCAATAACACATGGATCCGCTGGGTCCCAG-3′), respectively, with the mutagenic residues underlined. The *MFA1* template was pSM233 and the resultant mutant plasmids were designated pSM309 and pSM255. To construct a mutant in which the portion of *MFA1* corresponding to the mature **a**-factor coding sequence was deleted, a 0.9-kb *Bam*HI–*Xba*I fragment was deleted from pSM309 and replaced with the analogous *Bam*HI–*Xba*I fragment from pSM255. By this reconstitution, resulting in pSM291, the mature **a**-factor coding sequence is precisely deleted (Δ21–32) and is replaced by the DP codon pair.

We generated versions of *MFA1* in which one of two epitope tags (E1 or hemagglutinin [HA]) was inserted into, or substituted for, the mature coding sequence of **a**-factor. To generate a *Bam*HI-ended E1 epitope tag sequence, *Bam*HI sites were introduced by oligonucleotide mutagenesis into a C-terminal portion of the coronavirus E1 glycoprotein coding sequence, by using plasmid p57–6 (Machamer and Rose, 1987) as the template. The amino acid sequence of the *Bam*HI-ended E1 epitope tag is DPMFVYAKQSVDTGELESVATGGSSLYTMDP. A synthetic peptide corresponding to this sequence (minus the flanking DP codons) had been previously used to generate polyclonal antiserum (Machamer and Rose, 1987). The resulting *Bam*HI-ended E1 tag was subcloned into pRS316 (Sikorski and Hieter, 1989) yielding pSM224, which was used as the source of the E1 tag in the subsequent clonings. To generate a version of *MFA1* with the E1 epitope inserted within mature **a**-factor, the E1-containing *Bam*HI fragment from pSM224 was subcloned into pSM255 at the *Bam*HI site preceding codon 32, yielding pSM241. To generate a version of *MFA1* in which the mature **a**-factor amino acids are replaced by the E1 epitope tag, the *Bam*HI fragment from pSM224 was subcloned into pSM291 to yield pSM319.

To work with the HA tag, the HA epitope sequence was encoded as a pair of single-stranded complementary oligonucleotides (oSM42, 5′-GATCCAATGTACCCATACGATGTTCCAGATTACGCA-3′, and oSM43, 5′-GATCTGCGTAATCTGGAACATCGTATGGGTACATTG-3′) terminating with *Bam*HI sites. These oligonucleotides were annealed to each other to generate the double-stranded coding sequence for HA (flanked by *Bam*HI sites; DPMYPYDVPDYADP; Field *et al.*, 1988). The annealed duplex was ligated into the *Bam*HI site preceding codon 32 of pSM255 to yield pSM357.

Metabolic Labeling, Immunoprecipitation with a-Factor Antiserum, and SDS-PAGE Analysis

Pulse-chase and steady-state metabolic labeling with 150 μCi of [^{35}S]cysteine (1075.0 Ci/mmol, New England Nuclear, Boston, MA),

Table 2. Plasmids used in this study

Plasmid	Vector	Yeast marker	MFA1 genotype[a]	Source
pSM219	2μ	*URA3*	*MFA1*	Chen *et al.* (1997)
pSM220	2μ	*LEU2*	*MFA1*	Chen *et al.* (1997)
pSM224	*CEN*	*URA3*	E1 epitope	Chen (1993)
pSM233	*CEN*	*URA3*	*MFA1*	Chen *et al.* (1997)
pSM241	2μ	*URA3*	*mfa1*::E1 (32)	Chen (1993)
pSM255	2μ	*URA3*	*mfa1*::DP (32)	Chen (1993)
pSM258	2μ	*URA3*	*mfa1*-ΔVIA (34–36)	Chen (1993)
pSM291	2μ	*URA3*	*mfa1*-Δ (21–32)	This study
pSM309	2μ	*URA3*	*mfa1*::DP (21)	This study
pSM316	2μ	*URA3*	*mfa1*-Δ1 (35)	Chen (1993)
pSM319	2μ	*URA3*	*mfa1*-(Δ21–32)::E1	This study
pSM357	2μ	*URA3*	*mfa1*::HA (32)	Chen (1993)
pSM463	2μ	*TRP1*	*MFA1*	Chen *et al.* (1997)
pSM464	*CEN*	*TRP1*	*MFA1*	Chen *et al.* (1997)
pSM490	2μ	*URA3*	*mfa1*-I23M	Chen *et al.* (1997)
pSM1235	*CEN*	*TRP1*	*mfa1*-A32S	This laboratory

[a]DP refers to the insertion of a 6-bp *Bam*HI recognition site that encodes Asp-Pro. E1 and HA are epitope tags described in the text. Number in parentheses indicates the codon just C-terminal to the site of insertion.

preparation of intracellular and extracellular fractions, and immunoprecipitation with **a**-factor rabbit polyclonal antiserum 9–137 or 9–497 were carried out as described (Chen *et al.*, 1997). These antisera were raised against the unmodified **a**-factor 12-mer peptide in separate rabbits (Chen *et al.*, 1997). Metabolic labeling with [^{3}H]-lysine was carried out by addition of 500 μCi of L-[4,5-^{3}H]lysine (92.0 Ci/mmol, Amersham, Arlington Heights, IL). In our previous studies, intracellular and extracellular proteins were always subjected to immunoprecipitation prior to the SDS-PAGE analysis. Herein, to optimize detection of AFRP in the culture medium, the extracellular fraction (combined from trichloroacetic acid precipitation of the culture fluid and the *n*-propanol tube wash (Chen *et al.*, 1997) was resuspended in sample buffer and examined directly without immunoprecipitation. The modified SDS-PAGE (16%) method previously described (Chen *et al.*, 1997) was used to analyze both the immunoprecipitated and nonimmunoprecipitated samples. Proper separation of proteins in the nonimmunoprecipitated extracellular fraction is extremely sensitive to overloading. Therefore, we standardly loaded 10-fold less of this material per lane than for immunoprecipitated samples to optimize resolution (extracellular material deriving from 0.1 OD_{600} U of cells versus 1.0 OD_{600} U, respectively).

Preparation of Amberlite XAD-2 Resin

The polystyrene resin Amberlite XAD-2 resin (Sigma, St. Louis, MO; lot number 51H0879) has previously been shown to adsorb **a**-factor from culture fluid (Strazdis and MacKay, 1982). The XAD-2 resin was prepared by washing with excess distilled H_2O and then with 2 volumes of *n*-propanol in batch, incubating overnight at 30°C. The washed resin was stored covered in *n*-propanol. Prior to use, it was washed with excess distilled H_2O and sterilized by autoclaving in distilled H_2O. It should be noted that different lots of XAD differ greatly in their capacity to adsorb AFRP, whereas all lots are efficient in adsorbing **a**-factor.

a-Factor Activity Assay

The **a**-factor activity was measured using the semiquantitative **a**-halo dilution assay (Berkower and Michaelis, 1993; Nijbroek and Michaelis, 1997). **a**-Factor preparations including the original culture medium, the *n*-propanol concentrate, and the HPLC fractions (see section below) were serially diluted in twofold increments into YEPD medium containing 250 μg/ml bovine serum albumin (BSA; YEPD-BSA) or 50% MeOH (similar results were obtained using either YEPD-BSA or 50% MeOH as the dilution solvent). Aliquots (2 μl) of each dilution were spotted onto a lawn on a YEPD plate spread with 10^6 cells of the *MAT*α *sst2* tester strain SM1086. The plate was incubated at 30°C for 24 h. The definition of 1 U/ml of **a**-factor activity is the lowest dilution that still causes a nonturbid **a**-halo on the *MAT*α *sst2* strain.

Generation of the ^{35}S-labeled a-Factor and AFRP Tracer

To produce ^{35}S-labeled mature **a**-factor and AFRP for use as radioactive tracer in the large-scale purification procedure described in the next section, 10 OD_{600} U of logarithmic-phase yeast cells were labeled in SC drop-out medium with 500 μCi [^{35}S]cysteine under steady-state conditions overnight. Labeled cells and culture fluid were separated by centrifugation at 13,600 × *g* for 1 min in a microcentrifuge. The cell pellet was discarded and the culture supernatant was recentrifuged to remove any remaining cells. The supernatant from the second spin was transferred to a new tube and the prepared Amberlite XAD-2 resin (see description above) was added to the supernatant to equal approximately one-tenth of the total volume. After incubation overnight, the supernatant was removed and material adsorbed on the XAD-2 resin was recovered by a 0.5-ml *n*-propanol (HPLC grade, Aldrich, Milwaukee, WI) wash. Material remaining bound to the original polypropylene labeling tube was also recovered by a 0.5-ml *n*-propanol wash. The two *n*-propanol washes were pooled and this material was used as radioactive tracer for purification of **a**-factor and AFRP by reverse-phase HPLC. For each liter of culture fluid from unlabeled cells, the culture fluid from 5 OD_{600} U of ^{35}S-labeled cells was added as tracer.

HPLC Purification of a-Factor and AFRP

The procedure used to separate **a**-factor and AFRP is modified from methods previously used to purify **a**-factor (Strazdis and MacKay, 1982; Anderegg *et al.*, 1988). To generate a large-scale preparation of extracellular **a**-factor and AFRP, a *MAT***a** strain carrying wild-type (WT) or mutant *MFA1* on a 2μ plasmid was grown to saturation in 5 ml of synthetic drop-out medium. One milliliter of the saturated culture was inoculated into 1 l of synthetic dropout medium in a 2-l culture flask, and the culture was grown at 30°C for 48 h with aeration (approximately 300 rpm) until the OD_{600} of the culture reached 5.0 U. Cells were removed by centrifugation at 4500 × *g* for 5 min and the culture supernatant was recentrifuged to remove any remaining cells. Since **a**-factor is present both in culture fluid and also adheres onto the surface of the flask, the original 2-l flask, in which the culture was grown, was washed several times with distilled H_2O and the cleared culture fluid was added back to the flask. One hundred ml of the prepared XAD-2 resin was added to the culture fluid and incubated at 30°C overnight with gentle agitation to allow adsorption of **a**-factor and AFRP to the resin. After adsorption, the culture fluid was removed. The material adhering to the XAD-2 resin and flask was released by addition of 100 ml of *n*-propanol, allowing incubation to proceed at 30°C overnight. The *n*-propanol eluate was dried in a speed-vacuum concentrator with heat. The dried material was resuspended in 0.5 ml of *n*-propanol and then the [^{35}S]cysteine-labeled **a**-factor or AFRP tracer, prepared as described above, was added along with 0.5 ml of H_2O (HPLC grade, J.T. Baker) to generate a 50% propanol solution. The resulting 1-ml 50% *n*-propanol suspension was centrifuged at 13,600 × *g* for two 5-min periods to remove insoluble material. The sample was applied to a semipreparative Vydac C_{18} reverse-phase HPLC column (5-μm particle size, 10 × 250 mm, The Nest Group, Southborough, MA) attached to a Waters model 510 HPLC system (Millipore, Bedford, MA) using Maxima 820 chromatography workstation software (Waters, Millipore). The mobile phases were solvent A, 0.1% trifluoroacetic acid (TFA; (HPLC grade, Pierce, Rockford, IL) in H_2O and solvent B, 0.085% TFA in MeOH (HPLC grade, J. T. Baker). The column was initially equilibrated with 70% solvent A: 30% solvent B. **a**-Factor and AFRP were eluted from the column at a constant flow rate of 3.0 ml/min according to the following stepped linear gradient: between 0 and 5 min, the gradient was kept at 70% A:30% B; between 5 and 45 min, the percentage of B was increased from 30% to 70% and that of the A was decreased from 70% to 30%; between 45 and 85 min, the percentage of B was increased from 70% to 90% and that of the A was decreased from 30% to 10%; between 85 and 95 min, the gradient is changed from 10% A: 90% B to 0% A: 100% B. The eluted materials were monitored for absorption at 219 nm.

A sample (5 μl) of each fraction (80 total) was diluted into 5 μl of YEPD-BSA medium, and 2 μl of each diluted fraction was screened for **a**-halo activity. The fractions showing **a**-halo activity were further diluted in 1:2 increments to quantify **a**-factor activity in each fraction. To detect the fractions containing **a**-factor and AFRP, aliquots (60 μl) of each fraction were dried in a speed-vacuum concentrator, the dried material was resuspended in 5 μl of 1× Laemmli sample buffer, and samples were analyzed by SDS-PAGE in 16% gels.

Plasma Desorption Mass Spectrometry

One-tenth of each HPLC fraction, containing either **a**-factor or AFRP, was dried in the speed-vacuum concentrator and redissolved in 10 μl of 50% methanol. The sample solution was then deposited

on nitrocellulose-coated Mylar-backed aluminum foil (Applied Biosystems, Foster City, CA). After the sample solution was absorbed by the nitrocellulose (approximately 5 min), the sample foil was spin dried, followed by a microspin washing with 10 μl of 0.1% TFA. The plasma desorption mass spectra were recorded on a BIO-ION Nordic (Uppsala, Sweden) BIN-10K plasma desorption time-of-flight mass spectrometer, equipped with a 10-μCi $^{252}Cf_{98}$ (Californium-252) ionization source. Spectra were collected by a PDP 11–73-based BIO-ION data system. Positive ion spectra were recorded with an accelerating voltage of +20 kV to present number of primary events (2 to 9 million) depending on the quality of each individual spectrum. H^+ and Na^+ (or NO^+) ions were used for mass calibration. The margin of error in these measurements is 0.1–0.2%, which is 1–2 Da per 1000.

RESULTS

Identification of a Novel a*-Factor Related Peptide (AFRP)*

We previously characterized **a**-factor biosynthetic intermediates by metabolic labeling, immunoprecipitation, and SDS-PAGE analysis (Chen *et al.*, 1997); in those studies we detected a novel **a**-factor species that was present in the nonimmunoprecipitated extracellular fraction. This species was also detectable occasionally, only under certain conditions, in immunoprecipitated samples from both the intracellular and extracellular fractions. In the present study, we pursued the identification and characterization of this **a**-factor-related species. To visualize this novel species, strains expressing the **a**-factor gene *MFA1*, or lacking **a**-factor altogether (*mfa1*Δ *mfa2*Δ), were labeled with [^{35}S]cysteine under steady-state conditions and separated into intracellular and extracellular fractions. Immunoprecipitation using **a**-factor antiserum 9–137, followed by SDS-PAGE reveals the expected intermediates (Figure 1, lanes 1 and 2), which are the partially processed precursor species (P1 and P2) and the fully processed mature (M) **a**-factor (Chen *et al.*, 1997). However, when total proteins from the culture medium were examined without immunoprecipitation, along with **a**-factor itself, an additional [^{35}S]cysteine-labeled species was observed that had a slightly faster electrophoretic mobility than that of mature **a**-factor (Figure 1, lane 3). It should be noted that a faint band corresponding to this species is also detectable in the intracellular immunoprecipitate (lane 1). Because this molecule was only found in cells carrying the *MFA1* gene but not in cells deleted for the **a**-factor genes (Figure 1, compare lanes 3 and 6), it seemed highly likely that this rapidly migrating species is derived from the *MFA1* gene. We have designated this species AFRP, for **a**-factor-related peptide (AFRP). Because AFRP is metabolically labeled by [^{35}S]cysteine and because there is only a single cysteine residue at the C terminus of the *MFA1* gene, we hypothesized that AFRP must be derived from the C-terminal portion of the **a**-factor gene.

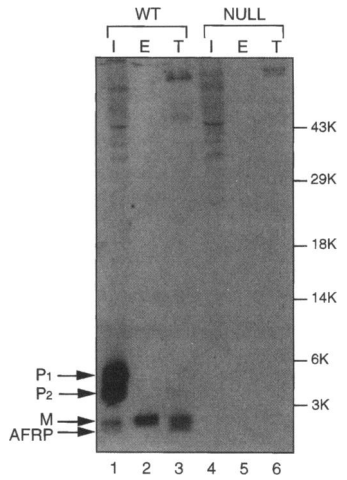

Figure 1. Identification of AFRP. Cells were labeled with [^{35}S]cysteine under steady-state conditions for 1 h. Intracellular (I; lanes 1 and 4) and extracellular (E; lanes 2 and 5) fractions were immunoprecipitated with **a**-factor antiserum 9–137 and analyzed by SDS-PAGE on 16% gels. The extracellular fraction was also examined without immunoprecipitation to assess the total protein profile (T; lanes 3 and 6). The strains labeled are SM1229 (Δ*mfa1*, Δ*mfa2*) containing the plasmid pSM464 (*CEN MFA1*) (WT) or no plasmid (NULL). The **a**-factor species P1, P2, and M and AFRP are indicated on the left; molecular weight markers are shown on the right.

AFRP was also observed when the *MFA1* gene was expressed from the chromosome, instead of from a plasmid, indicating that appearance of AFRP does not result from overproduction of the **a**-factor gene. Likewise strains expressing solely *MFA2* also generate AFRP, demonstrating that it can be generated from either of the **a**-factor precursors (our unpublished results). Moreover, AFRP was present in the culture medium of several *Saccharomyces cerevisiae* strains with distinctively different genetic lineages from our strain background; thus production of AFRP is not a strain-specific phenomenon (our unpublished results).

To analyze AFRP biosynthesis kinetically and to compare the rate of its formation and export with that of mature **a**-factor, we carried out a pulse-chase experiment in which immunoprecipitated and nonimmunoprecipitated samples were analyzed (Figure 2). AFRP is evident both in the intracellular immunoprecipitated and extracellular nonimmunoprecipitated fractions, but not in the extracellular immunoprecipitated fraction, as was also the case in Figure 1. The reason for the low immunoreactivity seen for AFRP in the extracellular immunoprecipitated sample is not clear but may in part be due to a difference in the composition between intracellular and extracellular AFRP that could influence antibody recognition, as discussed below. Overall, the kinetics of formation and export of AFRP are strikingly similar to those of mature **a**-factor. The formation and export of both species are rapid, with processing completed within 5 min

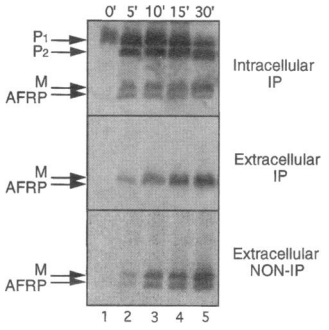

Figure 2. Kinetic analysis of AFRP biosynthesis. Cells were pulse labeled with [^{35}S]cysteine for 2 min and chased for the indicated times. Immunoprecipitated (IP) intracellular and extracellular fractions and the nonimmunoprecipitated (NON-IP) extracellular fractions were analyzed by SDS-PAGE on 16% gels. The **a**-factor antiserum used for immunoprecipitation was 9–497. The **a**-factor species are indicated. The strain labeled is SM1058 containing the plasmid pSM219 (2μ *MFA1*).

and export within 10–15 min. Approximately equal amounts of mature **a**-factor and AFRP are generated. The similarity in the kinetic parameters, and in the amounts of AFRP and **a**-factor that are generated and exported, suggests that their formation and exit from the cell occur concurrently.

C-Terminal Farnesylation, but not Methylation, Is Required for the Production and Export of AFRP

To determine whether C-terminal modification is critical for AFRP production, an **a**-factor deletion strain carrying a WT *MFA1* plasmid or the *mfa1* CAAX mutants ΔI35 and ΔVIA(34–36) were examined. In addition, *ram1*, *ram2*, and *ste14* mutant strains were examined. Cells were labeled with [^{35}S]cysteine and analyzed for **a**-factor and AFRP production (Figure 3). Both species, mature **a**-factor and AFRP, were produced from the strain expressing WT *MFA1* (lanes 1 and 7). In contrast, neither **a**-factor nor AFRP were found in the *mfa1-ΔI35*, *mfa1-ΔVIA(34–36)*, *ram1*, or *ram2* mutants, all of which are blocked for the farnesylation of the **a**-factor precursor (Powers *et al.*, 1986; He *et al.*, 1991; Sapperstein *et al.*, 1994; Chen *et al.*, 1997). Rather, only the unmodified **a**-factor precursor, P0, was apparent in these strains (Figure 3, lanes 2–5). Thus, farnesylation of the CAAX cysteine residue is critical for the production of AFRP, as well as for the production of mature **a**-factor.

Both mature **a**-factor and AFRP are generated intracellularly in a *ste14* mutant in which the C-terminal methylation of **a**-factor is blocked (Figure 3, lane 6; Sapperstein *et al.*, 1994). Interestingly, however, the unmethylated **a**-factor and AFRP formed in the *ste14* mutant exhibit a distinctive difference from one another. Although **a**-factor is absent in the culture medium of a *ste14* mutant, as has been seen previously (Sapperstein *et al.*, 1994), AFRP is present (Figure 3, lane 6). Thus, unmethylated AFRP can apparently be exported, whereas unmethylated **a**-factor cannot be (Sapperstein *et al.*, 1994). Therefore, although **a**-factor

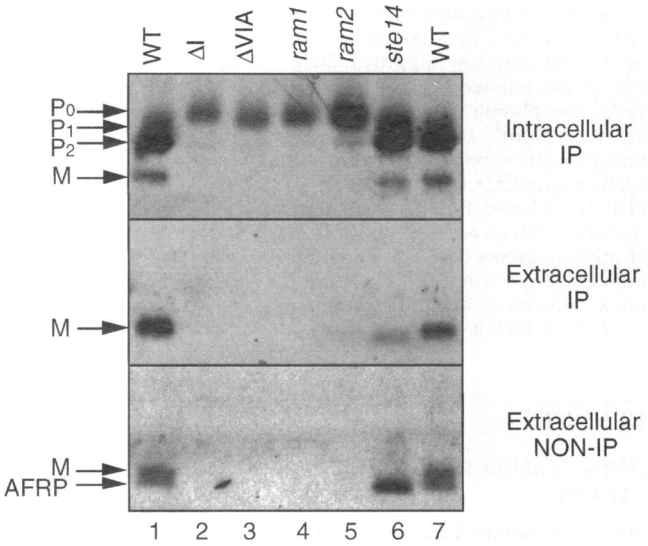

Figure 3. Analysis of AFRP biosynthesis in mutants affecting the C-terminal modification of **a**-factor. Cells were pulse labeled with [^{35}S]cysteine for 5 min. Intracellular and extracellular immunoprecipitates (IP) generated with **a**-factor antiserum 9–137 and the extracellular nonimmunoprecipitated (NON-IP) samples were analyzed by SDS-PAGE on 16% gels. Strains examined in lanes 1–3 and 7 are SM1458 (Δ*mfa1*, Δ*mfa2*) carrying the following WT or CAAX mutant plasmids: pSM219 (*MFA1*) (WT, lanes 1 and 7), pSM316 (*mfa1-ΔI35*, lane 2), or pSM258 (*mfa1-ΔVIA*, lane 3). Strains examined in lanes 4–6 are the chromosomal mutants SM1866 (Δ*ram1*), SM1863 (*ram2–1*), and SM1188 (Δ*ste14*), all carrying the WT *MFA1* plasmid pSM219.

and AFRP share a requirement for farnesylation for their formation, they are distinctive in terms of exit from the cell: methylation is required for the export of **a**-factor but dispensable for the export of AFRP.

AFRP Production Does Not Require the N-Terminal Proteolytic Cleavages Mediated by Ste24p and Axl1p that Generate Mature a-Factor

Because AFRP appears to be smaller than mature **a**-factor, based on its more rapid gel mobility, AFRP could be derived either from the mature (M) or a precursor (P1 or P2) form of **a**-factor. To directly determine the precursor of AFRP, we examined the N-terminal **a**-factor processing mutants, *ste24-Δ1* (defective in P1 → P2 conversion; Fujimura-Kamada *et al.*, 1997), and the *axl1 ste23* double mutant (defective in P2 → M conversion; Adames *et al.*, 1995). In these mutants the amount of mature **a**-factor (M) that is generated is either greatly diminished or abolished, respectively. As shown in Figure 4, AFRP is present at normal levels in both mutants, even though mature **a**-factor is highly reduced or absent altogether (Figure 4, compare lanes 2 and 3 with 1 and 4). In a separate experiment, we analyzed a *cis*-acting mutant *mfa1-ΔNY(21–22)*, in which the cleavage that generates ma-

ture **a**-factor is blocked; again, we found that AFRP production is unaffected (our unpublished results). The observation that AFRP is present in normal amounts in a *ste24*Δ mutant that is blocked for conversion of P1 → P2 suggests that AFRP is generated directly from the **a**-factor precursor species P1, which is C-terminally modified and has an intact N terminus.

AFRP Is Derived from the C-Terminal Portion of MFA1 Gene

To further examine the hypothesis that AFRP is directly derived from the C-terminal portion of *MFA1*, an **a**-factor deletion strain carrying a 2μ *MFA1* plasmid was metabolically labeled with either [^{3}H]lysine or [^{35}S]cysteine, and their labeling pattern was compared. Lysine is present near the N terminus of mature **a**-factor, at position 4 of 12 (see Figure 13). As expected, when intracellular immunoprecipitated **a**-factor was analyzed, both mature **a**-factor and AFRP were detected from cells labeled with [^{35}S]cysteine (Figure 5, lane 1). In contrast, using [^{3}H]lysine, only mature **a**-factor, and not AFRP, was detected (Figure 5, lane 2). This differential labeling phenomenon is consistent with the hypothesis that AFRP contains only the C-terminal portion, and not the N-terminal portion, of mature **a**-factor.

Purification of a-Factor and AFRP from Culture Medium

To determine the structure of AFRP, we purified **a**-factor and AFRP from yeast culture fluid. An **a**-factor deletion strain carrying a high-copy-number *MFA1* plasmid was used because it produces 10-fold more **a**-factor and AFRP than strains bearing only the chromosomal **a**-factor genes (Chen *et al.*, 1997). The purification steps used in this study are a modification of previously published procedures (Strazdis and MacKay, 1982; Betz *et al.*, 1987), designed for the concentration of mature **a**-factor.

Clarified culture medium was exposed to Amberlite XAD-2 polystyrene beads to adsorb **a**-factor and AFRP. Adsorbed material was eluted in 100% *n*-propanol. The eluted material was subjected to C_{18} reverse-phase HPLC chromatography using a stepped linear MeOH gradient (see MATERIALS AND METHODS for details). Each fraction was monitored by the **a**-factor halo activity assay (Figure 6A) and by SDS-PAGE (Figure 6B). For the latter purpose, a small amount of [^{35}S]cysteine-labeled radioactive tracer was added to the Amberlite bead eluate.

The XAD-2 bead adsorption yields approximately 50% of the original activity, as judged by the **a**-factor activity assay. Upon HPLC fractionation, **a**-factor activity was predominantly found in fraction 62 (Figure 6A). Likewise SDS-PAGE analysis indicates that mature [^{35}S]cysteine-labeled **a**-factor is present primarily in fraction 62 (Figure 6B) correlating with the **a**-factor activity assay. Labeled AFRP was detected mainly in fractions 54 and 55, although some of AFRP-sized species were found in fractions 58 and 59 (and possibly fraction 64, although the migration of this species is not precisely the same as for AFRP; Figure 6B). Little or no **a**-factor activity was found in any of the fractions containing AFRP. We also tested **a**-halo inhibitory activity in these fractions by adding AFRP to **a**-factor and carrying out **a**-factor halo dilution assays; however, no inhibitory activity was detected (our unpublished observations). Overall, a 30-fold purification of **a**-factor and AFRP was achieved by this two-step preparation, with the yield of **a**-factor representing 10–20% of the original activity in the culture medium. (At least part of the loss during purification can be attributed to the very "sticky" nature of **a**-factor and AFRP, which results in their adherence to the walls of glass and polypropylene vessels.) The material obtained by the above procedure is sufficiently pure for subsequent PDMS analysis (below).

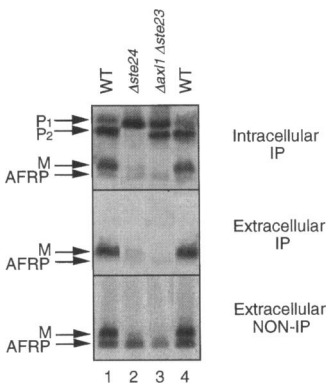

Figure 4. Analysis of AFRP biosynthesis in the two mutants defective in the N-terminal cleavage steps that generate mature **a**-factor. Cells were pulse labeled with [^{35}S]cysteine for 5 min and chased for 15 min. Intracellular and extracellular **a**-factor immunoprecipitates and the nonimmunoprecipitated extracellular fraction were analyzed by SDS-PAGE on 16% gels. WT and mutant strains defective for the conversion of P1 → P2 and P2 → M are examined; SM1058 carrying pSM219 (2μ *MFA1*, WT), lanes 1 and 4; SM3103 (*ste24*Δ) carrying pSM219, lane 2; and SM3256 (*axl1*Δ *ste23*Δ) carrying pSM219, lane 3.

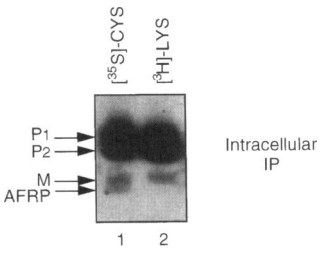

Figure 5. Detection of **a**-factor but not AFRP after metabolic labeling with [^{3}H]lysine. Strain SM1229 carrying a WT *MFA1* plasmid (pSM463) was pulse labeled with [^{35}S]cysteine or [^{3}H]lysine, for 15 min. Intracellular immunoprecipitates were analyzed by SDS-PAGE on 16% gels and autoradiography.

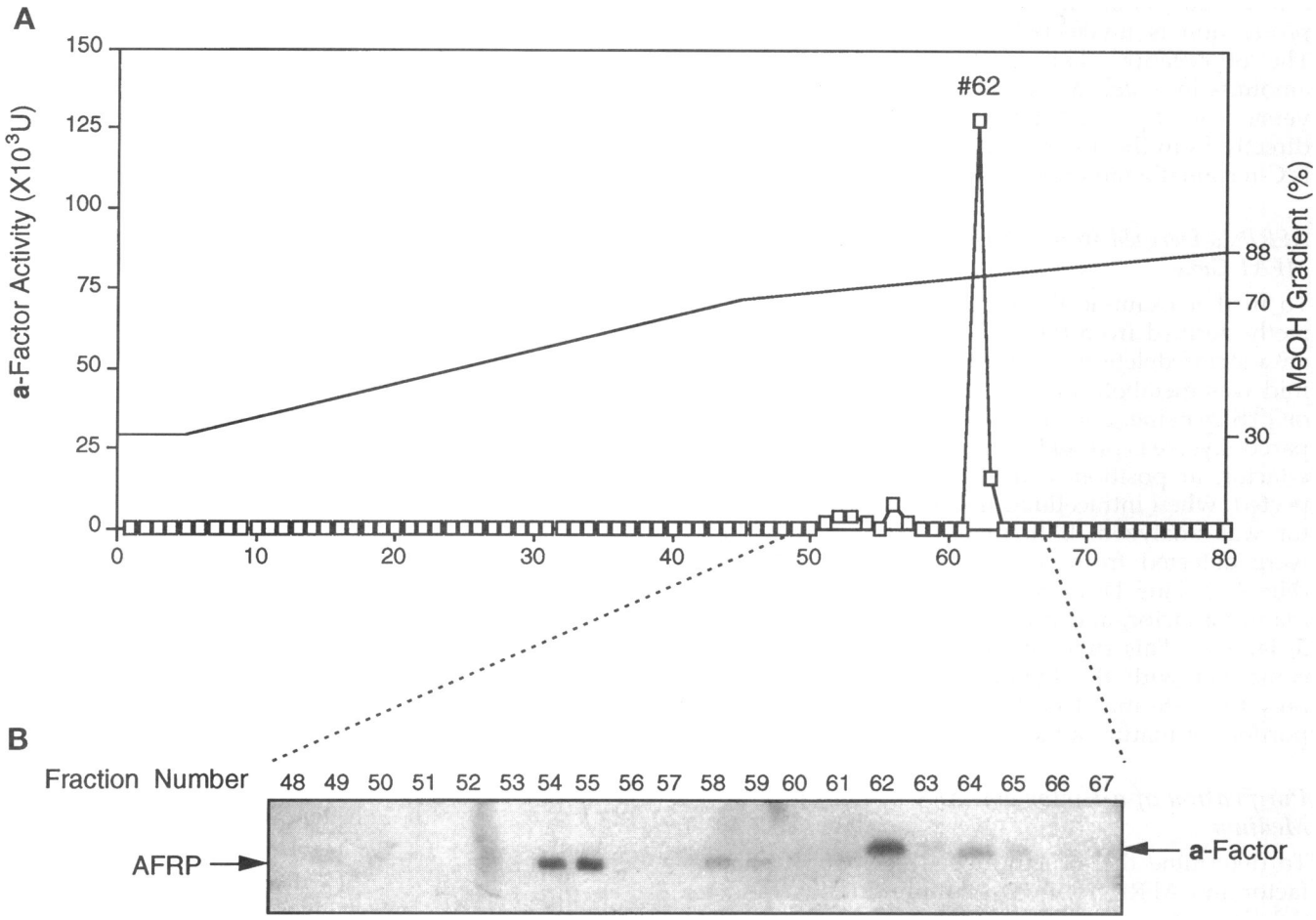

Figure 6. Purification of **a**-factor and AFRP by C_{18} reverse-phase HPLC. Prior to purification, **a**-factor and AFRP were concentrated from the culture fluid of unlabeled **a** cells (1 l of SM1229 containing pSM463 [*MFA1*]) by adsorption to XAD-2 resin and elution with *n*-propanol, as described in MATERIALS AND METHODS. The [^{35}S]cysteine-labeled culture fluid derived from 5 ml of the same cells, also prepared by adsorption onto XAD-2 resin followed by *n*-propanol elution, was added to the large-scale preparation as a radiolabeled tracer. The combined *n*-propanol eluate was fractionated on a C_{18} reverse-phase HPLC column, using a 30–100% MeOH gradient (diagonal line in A). (A) **a**-factor activity assay of the C_{18} reverse-phase HPLC fractions 1–80, assayed by the halo dilution method and quantitated (□) as described in MATERIALS AND METHODS. To directly determine the fractions containing **a**-factor and AFRP, aliquots (60 μl) of HPLC fractions 1–80 were dried, resuspended in 5 μl of 1× Laemmli sample buffer, and analyzed by SDS-PAGE on 16% gels and autoradiography. (B) Fractions 48–67, in which labeled tracer was detected, are shown. The positions of **a**-factor and AFRP on SDS-PAGE are indicated. These data are from a single purification (purification 1).

PDMS Analysis of Mature a-Factor and AFRP: Cleavage Occurs between G26 and V27

The experiments discussed in the sections above indicate that AFRP is derived from the C-terminal portion of the **a**-factor precursor. To determine the precise composition of AFRP, HPLC fractions containing AFRP and **a**-factor were analyzed by PDMS (Macfarlane, 1981). **a**-Factor and AFRP from several indepen-

Figure 7 (facing page). PDMS analysis of HPLC fractions containing **a**-factor or AFRP. Results of the PDMS analysis of HPLC-purified **a**-factor (fraction 62) and AFRP (fraction 54) from one purification (purification 1; Figure 6) are shown in A. The ordinate corresponds to intensity and the abscissa to the mass-to-charge ratio (m/z). In general, the observed peak corresponds to the mass of the species plus the mass of a proton [M+H$^+$]. In the **a**-factor fraction (left), there is a major molecular ion of m/z 1630, which correlates with the predicted mass of mature **a**-factor (1629 Da), and a minor molecular ion of m/z 1425. The difference between these two ions is 205 Da, which corresponds to the mass of a farnesyl group. In the AFRP fraction (right), a major molecular ion of 1072 is apparent. (B) Results of PDMS analysis of **a**-factor and AFRP from a separate purification (purification 2). Similar molecular ions were detected as those described in A, except that an additional molecular ion (867) was observed in the AFRP sample, which corresponds to the loss of farnesyl (205 Da) from AFRP. (C) Structure and calculated mass [M+H$^+$] of **a**-factor and AFRP.

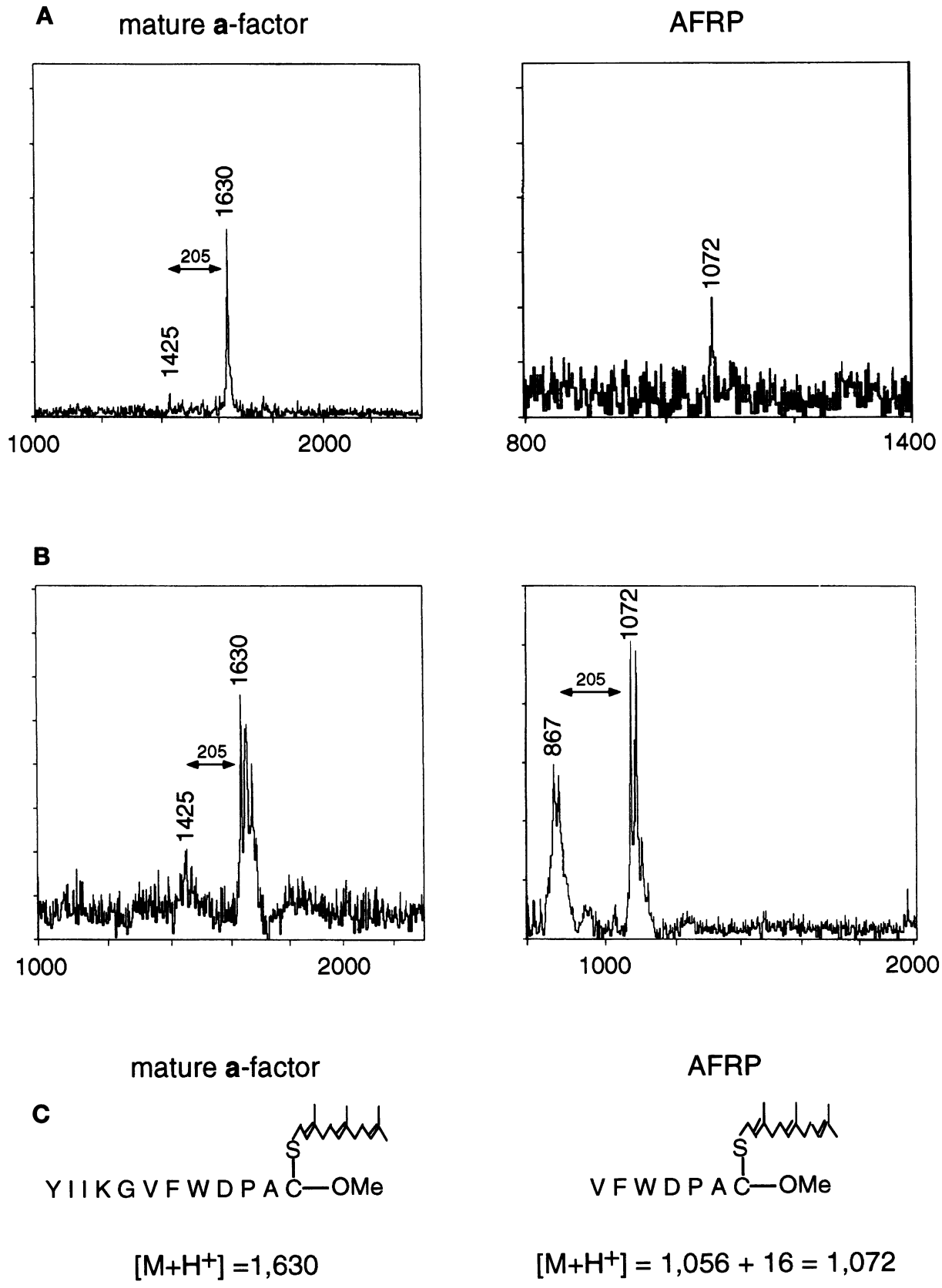
A
mature a-factor
AFRP
1630
205
1425
1072
1000
2000
800
1400
B
1630
205
1425
1072
205
867
1000
2000
1000
2000
mature a-factor
AFRP
C
S
Y I I K G V F W D P A C—OMe
S
V F W D P A C—OMe
[M+H+] =1,630
[M+H+] = 1,056 + 16 = 1,072

Figure 7.

dent HPLC preparations were examined; the spectra from two of these are shown (Figure 7, A and B). The position of the peaks along the horizontal axis represents their mass-to-charge ratio (m/z), and the mass of each species is equivalent to its molecular weight plus a proton (+1). In one preparation, the PDMS spectrum of the **a**-factor fraction contains a major protonated molecular ion peak with a mass-to-charge ratio (m/z) of 1630 and a minor peak of m/z 1425 (Figure 7A, left). In another preparation, the same **a**-factor ions (a major peak of 1630 and a minor peak of 1425 [Figure 7B, left]) were detected, although the latter spectrum exhibited a spread of species clustered around the peaks. The molecular weight of **a**-factor determined previously is 1629 Da (Anderegg *et al.*, 1988). The major ion $[M+H]^+$ (m/z 1630) observed corresponds well to this number as it represents the addition of a positively charged proton (m/z 1) to **a**-factor (m/z 1629). Interestingly, the difference between the major and the minor peaks is 205 Da, which matches the mass of a farnesyl group ($C_{15}H_{25}$). Therefore, the peak of m/z 1425 is most likely a fragment ion representing defarnesylated **a**-factor formed during mass spectrometry, as previously observed (Anderegg *et al.*, 1988).

When the AFRP fractions from the two independent preparations were analyzed by PDMS, we detected a single ion of m/z 1072 from one preparation (Figure 7A, right) and a pair of ions of m/z 1072 and 867 from the other (Figure 7B, right). As indicated in Figure 7C, the peak of 1072 Da corresponds to the seven C-terminal amino acids of **a**-factor including the farnesyl and methyl groups, plus an extra 16 Da. This structure of AFRP indicates that it must be generated by a proteolytic cleavage between residues G26 and V27 of the *MFA1* gene. In the AFRP fraction exhibiting two ions (Figure 7B, right), the difference between the major and minor peaks 1072 and 867, respectively, is 205 Da, correlating with the loss of a farnesyl group. For the AFRP and corresponding **a**-factor fractions derived from preparation 2 (Figure 7B), there are actually multiple AFRP species clustering around the major peak. The additional species that contribute to the width of this peak are in secondary peaks, 16 mass units apart, suggesting significant oxidation of this sample during purification. The lack of a defarnesylated ion in the first AFRP preparation (Figure 7A) may reflect the low abundance of the material that was analyzed (notice the signal-to-noise ratio is much lower than for the other spectra). This low abundance may be due to inefficient adsorption of AFRP to the nitrocellulose foil used for PDMS. We have observed that AFRP does not adhere to nitrocellulose of certain lot numbers. In contrast, **a**-factor does not exhibit this lot-specific variability in adherence to nitrocellulose.

Our hypothesis is that the extra 16 Da present in AFRP represents oxidation of AFRP, which is consistent with the previous observation that **a**-factor itself may become significantly oxidized during purification (Betz *et al.*, 1987). However, whereas the authors of the previous study suggested that oxidation might occur on the farnesyl group, we found that the defarnesylated ion for ***a***-factor (1425) and for AFRP (867) still bears the extra mass of 16 Da. This result indicates that oxidation does not occur on the farnesyl group, but most likely occurs within the peptide portion of AFRP. It is notable that although we detect both nonoxidized and oxidized **a**-factor ions, we have detected solely the oxidized form of AFRP.

PDMS Analysis of a-Factor and AFRP Produced by Two mfa1 Mutants

To further confirm the identity of AFRP and the cleavage site used to generate it, we sought to analyze **a**-factor and AFRP molecules derived from two *mfa1* mutants, A32S and I23M, respectively. According to the proposed structure (Figure 7C), the AFRP derived from *MFA1* is generated by a cleavage between G26 and V27. Therefore, the *mfa1*-A32S mutation should alter the mass of both **a**-factor and AFRP, whereas the *mfa1*-I23M mutation should alter the mass of **a**-factor but not of AFRP. Accordingly, we purified the **a**-factor and AFRP molecules produced by cells that carry plasmids bearing three different versions of *MFA1* (WT, A32S, or I23M). When **a**-factor fractions were subjected to PDMS, we detected major ions of m/z 1647 from the A32S mutant (Figure 8C) and m/z 1649 from the I23M mutant (Figure 8B), as compared with m/z 1630 for WT **a**-factor (Figure 8A). These observed ions precisely correlate with the mass shift predicted to result from the A32S and I23M mutations. The characteristic minor ions, corresponding to defarnesylated species, are also apparent in each case.

For AFRP fractions subjected to PDMS, the major ion detected from the A32S mutant has a m/z of 1088 as compared with WT AFRP, whose m/z is 1072 (Figure 8, C versus A). The difference corresponds to the replacement of alanine with serine in the mutant AFRP species. In contrast, the major ion detected from the I23M mutant is 1072 (Figure 8B), which is identical to WT AFRP. Therefore, the I23M mutation affects only **a**-factor but not AFRP and, thus, must lie outside of the region contained in AFRP. In summary, the PDMS analysis of **a**-factor and AFRP molecules derived from the *mfa1*-A32S and *mfa1*-I23M mutants provides compelling evidence that AFRP is generated from the C-terminal portion of the *MFA1* precursor; these findings are consistent with the conclusion that AFRP results from a cleavage between the residues G26 and V27.

It should be noted that ions corresponding to the defarnesylated forms of **a**-factor and AFRP were apparent in each case in Figure 8 and indeed provide a handy signature for their farnesylated counterparts. It

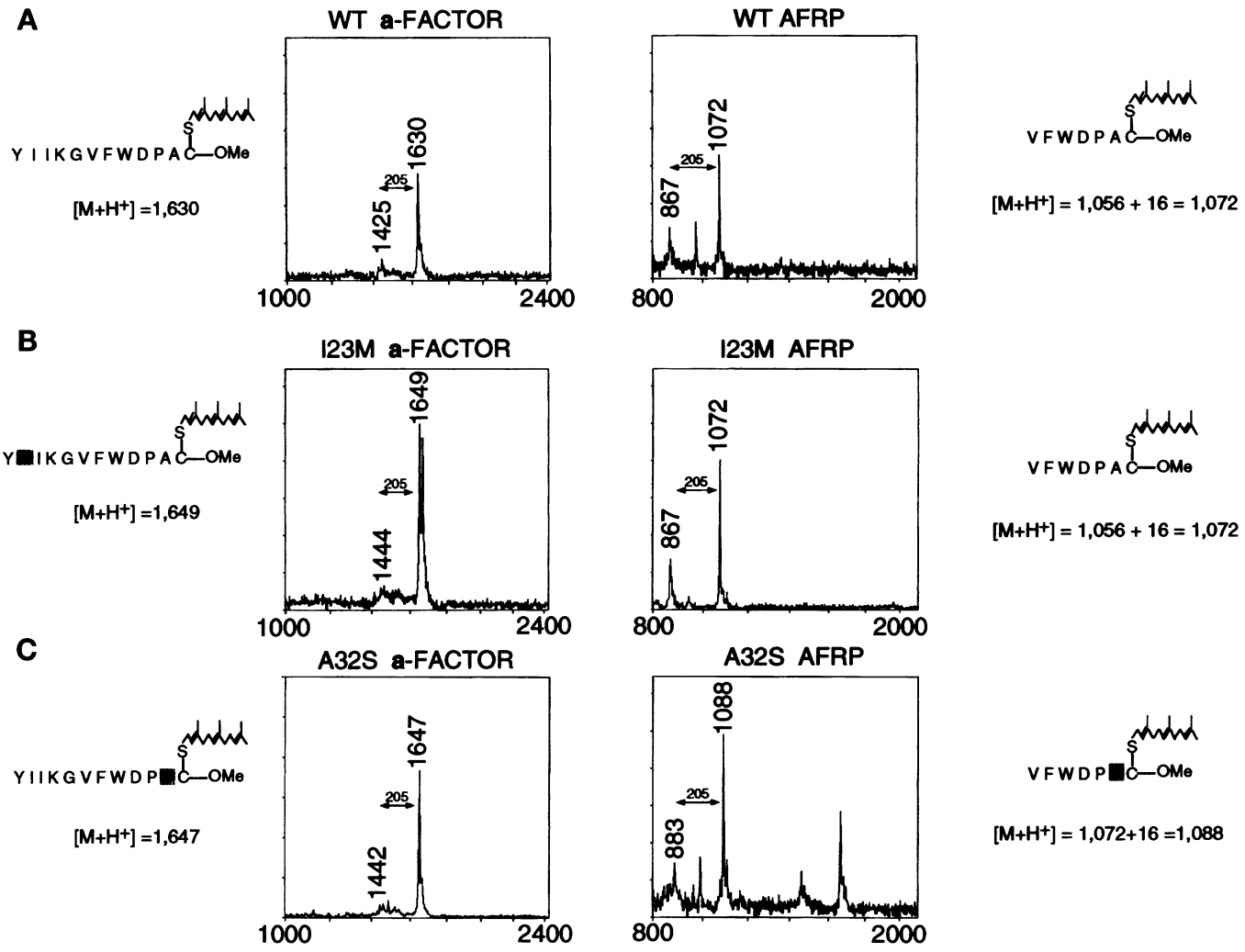

Figure 8. PDMS analysis of **a**-factor and AFRP derived from WT and mutant *MFA1*. PDMS analysis is shown for HPLC-purified **a**-factor and AFRP from strain SM1229 containing pSM463 (WT *MFA1*; A), pSM490 (*mfa1-I23 M*; B), and pSM1235 (*mfa1-A32S*; C). The major and minor molecular species are indicated. The difference (205 Da) between the major and minor molecular ions corresponds to the loss of a farnesyl group. The deduced structure and molecular weight are shown for each species. It should be noted that the unmarked species of higher mass (m/z 1663 and 1457) from the A32S AFRP spectrum represent the oxidized full-length **a**-factor derived from the A32S mutant and its defarnesylated counterpart and presumably are due to contamination of the PDMS run of the A32S AFRP.

is also worth pointing out that for the WT and A32S spectra of AFRP, an additional positive ion was observed in both cases (Figure 8A, m/z 973 between peaks 867 and 1072, and Figure 8C, m/z 989 between peaks 883 and 1088). This ion likely correlates with a loss of the N-terminal valine from the corresponding AFRP species and presumably occurs during PDMS.

AFRP Export Is Independent of the Ste6p Transporter

To determine whether the export of AFRP, like that of **a**-factor, is mediated by the Ste6p transporter, we compared the secretion of **a**-factor and AFRP in WT and *ste6* mutant strains. Cellular proteins were subject to steady-state metabolic labeling, separated into intracellular and extracellular fractions, immunoprecipitated (or not), and analyzed by SDS-PAGE (Figure 9). As expected, **a**-factor export occurs in WT cells and is blocked in the *ste6* mutant (Figure 9, top and bottom, compare lanes 1 and 4 to lane 2). Strikingly, however, in the case of AFRP, identical amounts were detected in the extracellular fraction of both the WT and *ste6* mutant strains (Figure 9, bottom, compare lanes 1 and 4 to lane 2). This experiment shows that, unexpectedly, and unlike mature **a**-factor, the export of AFRP is independent of Ste6p.

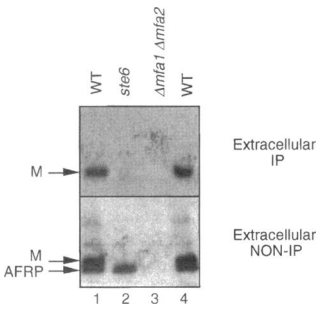

Figure 9. Comparison of **a**-factor versus AFRP export in a *ste6* mutant. Cells were labeled with [^{35}S]cysteine under steady-state conditions. Extracellular immunoprecipitates (IP) and the nonimmunoprecipitated extracellular fraction (NON-IP), analyzed by SDS-PAGE on 16% gels, are shown. Strains labeled are SM1458 containing pSM219 (*MFA1*) (lanes 1 and 4), SM1458 with no plasmid (lane 3), and SM1646 (Δ*ste6*) containing pSM220 (*MFA1*; lane 2).

The major export route used by most secreted proteins in the cell is the classical secretory pathway (Schekman, 1985; Pryer *et al.*, 1992). To examine whether the secretion of AFRP relies on this pathway, we examined the appearance of AFRP in the culture fluid in a set of temperature-sensitive *sec* mutants, *sec1*, *sec 7*, and *sec18*, that block the secretory pathway at discrete steps (Novick *et al.*, 1981). Our results indicate that the export of AFRP is not affected by the *sec* mutants (our unpublished observations), implying that AFRP does not require the secretory pathway for its formation or export.

Purification and PDMS Analysis of AFRP Secreted by a ste6 Mutant

To ensure that the structure of AFRP secreted by a *ste6* mutant does not differ from AFRP secreted by WT cells, we purified AFRP from the culture fluid of the *ste6* mutant using XAD2 beads, HPLC fractionation, and SDS-PAGE analysis. Like AFRP secreted from a WT strain, AFRP from the *ste6* mutant was also mainly found in fractions 54 and 55, with a small amount also present in fractions 58, 59, and 64 (Figure 10A). The major AFRP-containing fraction (fraction 55) was subjected to PDMS (Figure 10B). The positive ions observed were *m/z* 1072 and *m/z* 867, which are the same as those detected from a WT strain (Figure 7). Thus, the AFRP species secreted from a *ste6* mutant has the same structure as that of AFRP from a WT strain. The presence of a normal amount of AFRP in the culture fluid of a *ste6* mutant strain in which **a**-factor is entirely absent makes it unlikely that AFRP is derived from **a**-factor extracellularly, even in a WT strain.

Identification of AFRP-sized Molecules from Fusion Proteins

To analyze the specificity of the proteolytic events that generate AFRP we have constructed three epitope-tagged **a**-factor fusion proteins, designated fusion 1, 2, and 3 [*mfa1*::E1(32), *mfa1*::HA(32), and *mfa1*-Δ(21–32)::E1(32), respectively (Figure 11A)]. In these fusions, foreign amino acids are either added within (fusions 1 and 2) or substituted for (fusion 3) the mature region of *MFA1*. Strains expressing WT *MFA1* or the fusion proteins were metabolically labeled and extracellular extracts were examined by SDS-PAGE for the secretion of species derived from the fusion proteins. Although an **a**-factor-sized peptide is not apparent for the fusions (Figure 11B, compare lanes 3–5 with lanes 1 and 6), AFRP-sized molecules can be detected. These peptides are clearly dependent on the expression of

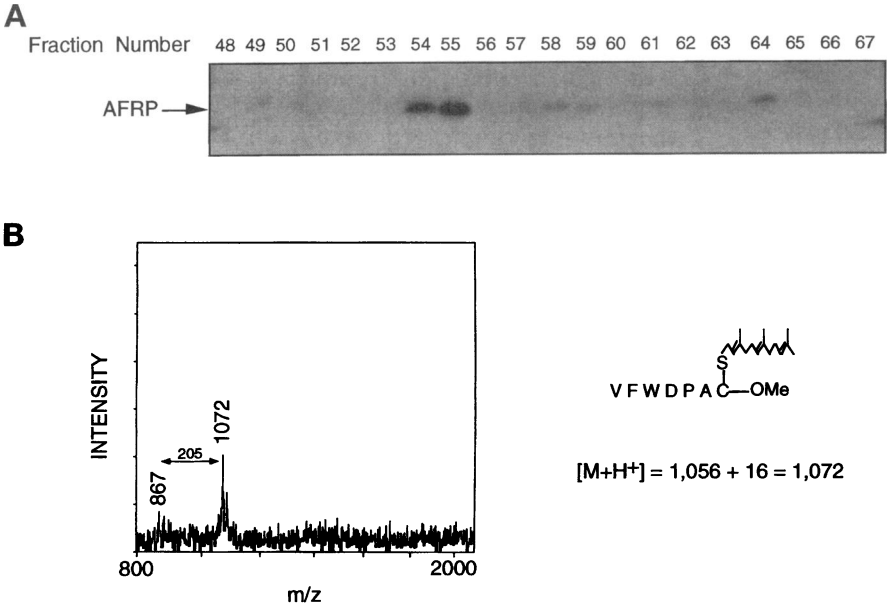

Figure 10. Purification and structural determination of AFRP from a *ste6* mutant. AFRP from SM1646 (Δ*ste6*) carrying pSM220 (*MFA1*) was purified from the culture fluid by absorption to the XAD-2 resin and reverse-phase HPLC. A large-scale nonradioactive sample and a labeled tracer sample were prepared from the same strain. In A, HPLC fractions 1–80 were analyzed by SDS-PAGE and only those fractions (fractions 48–67) containing a labeled species of the appropriate molecular weight are shown. (B) PDMS analysis of fraction 55, which contains the AFRP peak. The difference between the major molecular ion of 1072 and the minor ion of 867 corresponds to the loss of farnesyl (205 Da). The deduced structure of AFRP derived from the *ste6* mutant is also shown.

the gene fusions, because AFRP-sized species are lacking in cells that express neither WT or fusion forms of *MFA1* (Figure 11B, lane 2).

Because there is only one cysteine residue, located near the very C terminus of these fusion constructs, and because the AFRP-sized molecules can be labeled with [^{35}S]cysteine, the AFRP-sized species must derive from the C-terminal portion of the fusion proteins. If this hypothesis is correct, then the AFRP-sized peptides should have a very different amino acid sequence than authentic AFRP, sharing only its C-terminal farnesylmethylcysteine. Consequently, the proteolytic cleavage event that generates these species must occur within the E1 or HA epitopes to generate AFRP-sized molecules. This implies the existence of a protease(s) that is able to cleave peptide bonds regardless of the peptide sequence. One difference between the cells expressing the WT *MFA1* gene versus the fusion genes is that peptides migrating faster than WT AFRP were absent for WT, but present, in addition to the AFRP-sized peptides, for the fusion strains (Figure 11B, lanes 3–5). The identity of these species is addressed in the next section.

Purification and PDMS Analysis of the AFRP-sized Molecules Derived from Two Fusion Proteins

To determine the structure of the AFRP-sized molecules, fusion AFRPs from the culture fluid of an **a**-factor deletion strain carrying either fusion 1 [*mfa1*::E1(32)] or fusion 2 [*mfa1*::HA(32)] were HPLC-purified as described above, using the appropriate [^{35}S]cysteine-labeled tracer. The fractions containing AFRP-sized species from the fusions were detected by SDS-PAGE analysis (Chen, 1993). The major AFRP fraction (fraction 55) from fusion 1 [*mfa1*::E1(32)] was subjected to PDMS. As shown in Figure 12A, a group of peptides with m/z values of 949, 786, 685, 538, and 423 were observed, respectively (Figure 12A). If these are protonated species, then the molecular weights correlate with those calculated for a series of C-terminally farnesylated and methylated fusion peptides, ranging from 6 to 2 amino acids long. For fusion 2 [*mfa1*::HA(32)], PDMS analysis of the major AFRP-containing HPLC fraction (fraction 60) revealed a group of peptides with m/z values of 1199, 1084, 1000, 903, 624, and 569 (Figure 12B). These calculated molecular weights are consistent with those predicted for a series of C-terminally farnesylated and methylated fusion peptides ranging from 9 to 3 amino acids long. (It should be noted that the lack of 15 mass units [−15] for several species in Figure 12 is likely to correspond to loss of the methyl group, and the addition of 16 mass units [+16] is presumed to correspond to oxidation.) Presumably, the collection of AFRP-sized species made by fusions 1 and 2 reflect hetergeneity during the cleavage event that yields them. Alternatively, these smaller species may be generated by proteases in the culture fluid. The reason for the high level of fragmentation observed for the fusion-derived AFRP species, in contrast to the low level of fragmentation for **a**-factor-derived AFRP is not clear. From our findings, we can determine the presumed sites of cleavage used to generate the fusion-derived AFRPs. The sites from which the largest peptides are generated are between residues Leu and Tyr (fusion 1) and Tyr and Asp (fusion 2), in contrast to Gly and Val for true AFRP. Although the AFRP species derived from WT MFA1 and fusions 1 and 2 share a prenlyated methylated cysteine residue preceded by Asp-Pro, the remaining residues are not shared. Thus, the structural determination of these fusion AFRPs demonstrates that C-terminally farnesylated and methylated peptides can be generated and exported regardless of their peptide sequence, implying the possible existence of both novel processing and export mechanisms, distinct from those involved in the biogenesis of **a**-factor per se.

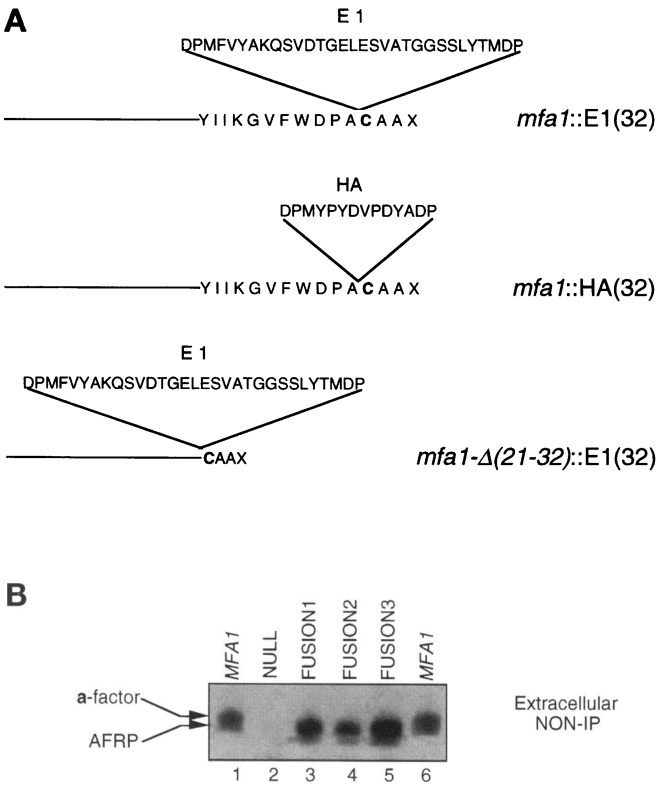

Figure 11. Identification of extracellular AFRP-sized molecules produced from fusion proteins. In A, the amino acid sequence of the E1 and HA epitope tags and their positions of insertion into the *MFA1* gene are shown. Note that the coding sequence corresponding to most of mature **a**-factor is deleted in fusion 3 (ΔY22-A32). In B, cells were labeled with [^{35}S]cysteine under steady-state conditions; the nonimmunoprecipitated (NON-IP) extracellular fraction was analyzed by SDS-PAGE on 16% gels. The strains labeled are SM1458 containing pSM219 (*MFA1*), pSM241 [*mfa1*::E1(32); fusion 1], pSM357 [*mfa1*::HA(32); fusion 2], and pSM319 [*mfa1*-Δ*21–32*::E1(32); fusion 3], or carrying no plasmid (null).

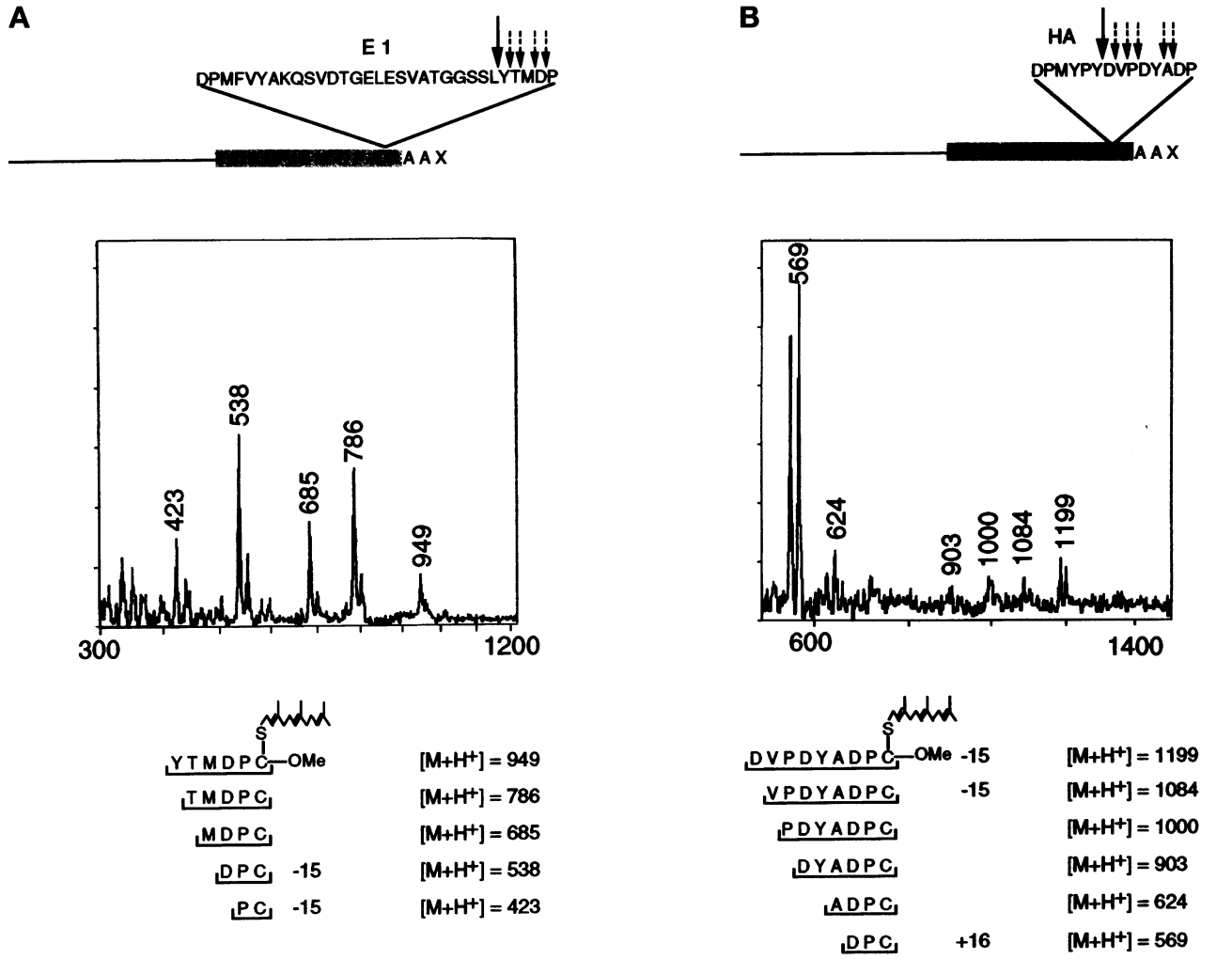

Figure 12. Purification and structural determination of AFRP-sized molecules from *mfa1*::E1 and *mfa1*::HA fusions. AFRP-sized molecules from strains expressing the *mfa1*::E1 (A) and *mfa1*::HA (B) fusions were purified from the culture fluid by adsorption to the XAD-2 resin and reverse-phase HPLC. HPLC fractions 1–80 were analyzed by SDS-PAGE and autoradiography. The fractions containing fusion AFRPs were detected by following the corresponding radiolabeled tracers. The peak fraction containing fusion AFRPs (fractions 55 and 60, respectively) were analyzed by PDMS. Several molecular ions are apparent. The deduced structures of the fusion AFRPs are shown below the spectrum; the sites of cleavage generating these species are indicated by arrows (above). Strains are SM1458 containing plasmids pSM241 (A) and pSM357 (B).

DISCUSSION

Comparison of the Biogenesis Pathway of a-Factor versus AFRP

In this study, we have identified and characterized a novel peptide secreted by *S. cerevisiae*. The production of this peptide, which we have designated AFRP (for **a**-factor-related peptide), is integrally related to the production of the **a**-factor mating pheromone. Purification and mass spectrometry of AFRP has revealed that it contains the same C-terminal seven amino acids as mature **a**-factor, including the farnesyl and carboxylmethyl modifications of cysteine (plus 16 additional mass units that are likely to result from the oxidation of an amino acid side chain). The presence of this alternative form of **a**-factor can explain, in part, one unexpected feature of **a**-factor biogenesis, namely, its apparent inefficiency (Chen *et al.*, 1997). We now know that a portion of the total amount of **a**-factor precursor that is synthesized by the cell is converted to AFRP instead of mature **a**-factor, thus accounting for some of the "missing" **a**-factor.

An important goal of the present study was to characterize the formation and export of AFRP. Figure 13 shows our model for the biogenesis of AFRP (right), as compared with that of **a**-factor (left). Three striking conclusions concerning the biogenesis of AFRP emerged

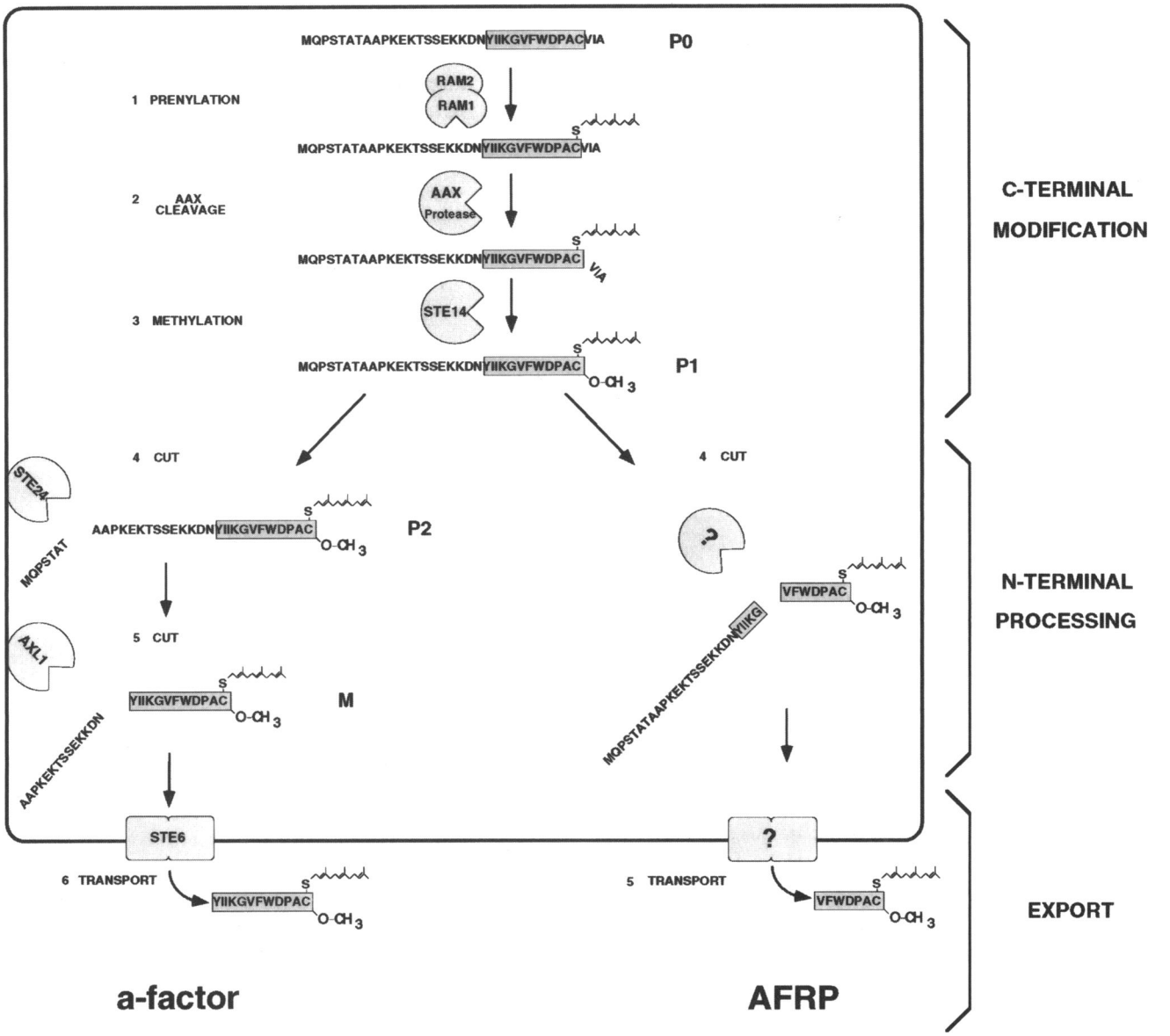

Figure 13. Comparison of the biogenesis and export of AFRP versus a-factor: a model. The biosynthetic intermediates of the **a**-factor precursor encoded by the *MFA1* gene are shown; these include precursor species (P0, P1, and P2), mature **a**-factor (M), and AFRP. The known cellular components that mediate **a**-factor biogenesis are indicated, as are components hypothesized to mediate the formation and export of AFRP. The C-terminal modification of the P0 precursor involves prenylation by Ram1-Ram2p, C-terminal cleavage of three residues by Rce1p and possibly Afc1p/Ste24p and carboxylmethylation by Ste14p, yielding P1. The data presented in this study indicate that the fully C-terminally modified precursor P1 is the common progenitor of both **a**-factor and AFRP. To yield **a**-factor (left), P1 undergoes two sequential cleavages at T7–A8 and N21–Y22 mediated by Ste24p and Axl1p, respectively, followed by export via Ste6p. To yield AFRP (right), P1 apparently undergoes a single cleavage at G26–V27 mediated by a postulated AFRP protease resulting in a prenylated and methylated 7-mer, identical to the C-terminal portion of mature **a**-factor. AFRP is exported in a Ste6p-independent manner by an unknown transporter or by diffusion. Because the identity of the AFRP protease and exporter are unknown, they are designated with question marks.

from our work: First, AFRP is derived from the **a**-factor precursor species P1 and not from mature **a**-factor. This conclusion is based on the finding that mutants (*ste24* and *axl1*) that cannot generate mature **a**-factor, due to an N-terminal processing defect, nevertheless generate AFRP normally. Thus, as indicated in Figure 13, the **a**-factor P1 precursor is subject to "alternative processing events" mediated by either Ste24p and Axl1p (left) or by the AFRP protease (right), leading to the formation of either mature **a**-factor or AFRP, respectively. Second, the AFRP protease may operate by a sequence-independent but length-specific mechanism, possibly using prenyl-

cysteine as a landmark from which to measure (see also below). This possibility is based upon the unexpected appearance of AFRP-sized molecules in the culture fluid of cells expressing fusion proteins containing foreign residues in place of authentic **a**-factor sequences. Third, and most strikingly, **a**-factor and AFRP appear to use different transporters to exit the cell: whereas the export of mature **a**-factor fails to occur in a *ste6*Δ mutant, the export of AFRP is unaffected. Furthermore, the carboxylmethyl group of **a**-factor, which is thought to be a critical recognition determinant for the Ste6p transporter (Sapperstein *et al.*, 1994), does not appear to be a critical determinant for AFRP secretion. This conclusion is based on our finding that although the export of **a**-factor is blocked in a *ste14* mutant, which is defective in carrying out carboxylmethylation, the export of AFRP is unaffected. This result provides further evidence that **a**-factor and AFRP use distinct export mechanisms.

The Export of AFRP Is Independent of the STE6 Transporter

Considering the structural similarity of AFRP and **a**-factor, it is unexpected and quite intriguing that AFRP is exported in a Ste6p-independent manner. What cellular machinery is responsible for the export of AFRP? Because the export of AFRP, like that of **a**-factor, is not impaired in *sec* mutants defective for secretion via the classical secretory pathway (our unpublished observations), it appears that AFRP, like **a**-factor exits the cell via an alternative route. It is interesting, therefore, to speculate that another ABC-type transporter may be responsible for the secretion of AFRP. Members of the the ABC superfamily of transporters have demonstrated a capacity to handle a broad range of substrates. For instance, the human multidrug-resistance protein can transport hydrophobic drugs that vary greatly in their chemical structure (Gottesman and Pastan, 1993). Likewise, the human TAP1/TAP2 pump can transport peptides with completely different amino acid sequences across the endoplasmic reticulum membrane for antigen presentation (Parham, 1992). Thus, given that the fusion-derived AFRP-sized molecules studied herein all appeared to be export substrates, even though they contain sequences distinctly different from one another and from authentic AFRP, an ABC superfamily member is a particularly compelling candidate for an AFRP transporter. We note that although our data does not rule out the possibility that AFRP and the AFRP-sized molecules derived from the fusion constructs could use distinct transporters, the possiblity of multiple transporters for these species seems unnecessarily complex.

Recently, we carried out a homology search of the completed genome sequence of *S. cerevisiae* to identify all potential ABC proteins (Michaelis and Berkower, 1995; Taglicht and Michaelis, 1997). We identified 30 ABC open reading frames, of which 22 (including Ste6p) are predicted to contain multiple membrane spans and are thus likely to function as true ABC transporters. Any of these could potentially function as an AFRP transporter, which can be tested by examining AFRP export in strains deleted for these genes or in strains overexpressing them.

It is also possible that a non-ABC type of transporter could be responsible for AFRP export. We have tested one such candidate, the nonclassical exporter Nce2p, which is a multiple membrane spanning protein that has been shown to mediate the transport, in yeast, of galectin, a mammalian nonclassical export substrate (Cleves *et al.*, 1996). Because AFRP is secreted normally in an *nce2–1* mutant, the Nce2p transporter is apparently not required for AFRP export (Nijbroek and Michaelis, unpublished data). Finally, it is theoretically possible that AFRP could exit the cell via simple diffusion. However, we feel that this is not likely in light of the finding that the export kinetics of AFRP and **a**-factor are strikingly similar (Figure 2); such similar kinetics of export would be unlikely if one molecule were exiting by diffusion and the other were undergoing active transport. Furthermore, there is increasing evidence that even small lipophilic molecules such as steroids, which were once thought to cross lipid bilayers unaided, can be assisted across membranes by transporters. This is exemplified by the efflux of steroid molecules such as dexamethasone from yeast by the Pdr5p transporter (Kralli *et al.*, 1995). It will, of course, be an interesting challenge to identify the AFRP transporter. However, because we do not presently have a simple assayable phenotype to follow, identification of such a component at this time would require brute force screening of candidate mutants using metabolic labeling followed by SDS-PAGE.

Specificity of the Protease that Generates AFRP

Prenylation appears to be a critical modification for the production of both **a**-factor and AFRP. We have previously shown that during the biogenesis of **a**-factor, C-terminal prenylation of the precursor is required for its membrane association and for subsequent N-terminal proteolytic processing to form mature **a**-factor (Chen *et al.*, 1997). Herein we demonstrate that prenylation is also a prerequisite for the formation of AFRP; since *mfa1*-CAAX mutants (ΔVIA, ΔI), or cellular prenylation-defective mutants (*ram1*, *ram2*), are unable to generate AFRP. One potential explanation for this prenyl requirement is that the AFRP protease (itself possibly membrane-associated, like the **a**-factor protease Ste24p) can encounter the precursor only when it is membrane-associated. Alternatively, or in addition, the prenyl group could serve as a specific recognition determinant or landmark for the AFRP protease.

One feature that the AFRP cleavage sites have in common in WT *MFA1* and in the fusion constructs is that they are close (9 amino acids or fewer) to the prenylated cysteine. Our fusion constructs contain an intact CAAX motif but have foreign amino acids adjacent to CAAX, instead of authentic **a**-factor residues. Unexpectedly, strains expressing these fusions secrete molecules of approximately the same size as AFRP whose amino acid composition corresponds to the newly introduced residues, instead of the authentic **a**-factor residues (Figures 11 and 12). Thus, an attractive possibility is that the AFRP protease recognizes prenylcysteine as a landmark and cleaves the substrate a relatively fixed distance away from it, independent of the sequence at the cleavage site. Alternatively, because it is likely that prenylcysteine serves as an anchor point in the membrane for **a**-factor, the AFRP protease could measure a particular distance from the membrane per se and cleave its substrate at that point. Indeed, one such proteolytic activity has been described that cleaves β-amyloid at a fixed distance from its membrane span, regardless of the amino acid residues that are present at the cleavage site (Sisodia, 1992).

In the analysis of AFRP derived from WT *MFA1* and from our fusion constructs, we observe sequence-independent cleavage, with cleavage occurring between unrelated pairs of amino acids: Gly-Val for AFRP, Leu-Tyr for fusion 1, and Tyr-Asp for fusion 2 (and perhaps other amino acid pairs if the smaller species we detect in Figure 12 are indeed generated intracellularly). Clearly, such a diverse processing pattern could not be achieved by a protease whose recognition sequence is highly specific. One candidate protease that could accomplish cleavage at multiple sites is the proteosome, since it is known to have multiple endopeptidase activities (Hochstrasser *et al.*, 1991; Hochstrasser, 1995). However, in a mutant defective for protease function (*pre1–1*), the production of AFRP is unaffected, indicating that the proteosome is not the AFRP protease (Choi and Michaelis, unpublished observation). We note that although we cannot rule out the possibility that cleavage of the fusion proteins is occurring by a different protease than the authentic AFRP-producing protease, there is no compelling reason to invoke two separate proteolytic activities.

In contrast to the AFRP protease, the **a**-factor proteases, Ste24p and Axl1p, show a high degree of substrate specificity, because mutations in residues flanking their cleavage sites can block processing (Fujimura-Kamada *et al.*, 1997; Nouvet, Kistler, and Michaelis, unpublished results). Yet for these proteases too, the distance of the cleavage site from prenyl cysteine may also be important, because cleavage by these proteases is significantly blocked by insertions that alter the distance between the prenyl cysteine of **a**-factor and the Ste24p or Axl1p cut sites (Nouvet and Michaelis, unpublished observations). Another C-terminally cleaved CAAX protein, mammalian nuclear lamin A, is initially C-terminally prenylated and methylated (Weber *et al.*, 1989). However, as part of its normal life cycle, its C terminus, including the prenylated methylated cysteine, is cleaved off. The lamin A protease is specific, like the **a**-factor proteases, because mutations flanking its cut site block its use (Hennekes and Nigg, 1994). An interesting model is that prenylcysteine serves as a recognition landmark for all proteases that act upon CAAX substrates. The AFRP protease, however, may be distinctive among these by virtue of its ability to cleave at many different residues.

In light of its lack of substrate specificity, it is reasonable to ask whether the AFRP protease could have a general cellular role for the cleavage of prenyl proteins unrelated to **a**-factor and AFRP, for instance acting upon Ras or the G protein γ subunit, which represent two important signaling molecules (Clarke, 1992). Cleavage by such a protease could serve a down-regulatory function by permanently inactivating these proteins. Alternatively, the AFRP protease may play an important general catabolic function. It is interesting to note that no cellular mechanism is presently known for the metabolic turnover of prenyl groups (Zhang and Casey, 1996); the thioether bond between the sulfur of cysteine and the farnesyl carbon is an extremely stable bond. Because prenylcysteine can neither be broken down for recycling nor be reused as is, to be cleared, it may instead need to be discarded from the cell. The AFRP protease in conjunction with the putative AFRP transporter could provide a way for cells to accomplish this task.

Kinetically, the formation of mature **a**-factor versus AFRP are similar, as determined by pulse-chase experiments. Operationally, there appear to be two different pools of P1 in the cell, one acted upon by the **a**-factor protease Ste24p and the other by the AFRP protease. Whether the content of these pools is determined stochastically or as the result of a particular conformation or location of a portion of the P1 precursor is not clear.

What Is the Physiological Role of AFRP?

Although the amount of AFRP that is exported from the cell is comparable to that of **a**-factor, the physiological role of AFRP is not known. Unlike **a**-factor, AFRP does not appear to possess either a significant stimulatory activity or an inhibitory activity: We detected nearly no activity by the halo assay, in which serial dilutions of AFRP are tested for their ability to mediate the growth arrest of *MATα* cells. Similarly, when we tested whether AFRP has an inhibitory role in mating, perhaps acting as an antagonist for the **a**-factor receptor, we did not detect an inhibition of mating resulting from the addition of exogenous AFRP to mating cells. These results are consistent with those of Becker and coworkers (Caldwell *et al.*, 1994), who examined the activity of chemically synthesized

versions of **a**-factor that were N-terminally truncated. One of the compounds tested by this group had precisely the composition of AFRP, except that it was presumably unoxidized. This compound exhibited a dramatically reduced activity when compared with **a**-factor (4000-fold reduced for growth arrest, and 125-fold reduced for mating restoration). Nevertheless it is interesting that in these studies it was possible to detect a low residual activity associated with synthetic AFRP. Presumably, with sufficiently high chemical quantities of this material, it is possible to reach a detection threshold where a very low level of activity can be observed. The AFRP that we purified appears to be oxidized, which may also lessen its activity. We do not know whether this oxidation occurs in vivo or whether it reflects an artifact of preparation. Indeed oxidation of mature **a**-factor has been seen in previous **a**-factor purification studies (Betz *et al.*, 1987), although its affect on mating has not been determined.

It remains possible that AFRP may have a role in mating. It is now known that high levels of pheromones are produced, indeed required, during the late stages in mating, in particular for cell fusion (Brizzio *et al.*, 1996). We have examined **a**-factor and AFRP production during the late stages of mating and indeed found that AFRP is produced at levels similar to that of **a**-factor (Choi and Michaelis, unpublished observations). However, it is presently difficult to assess the specific role of AFRP, as its production is inseparable from that of **a**-factor. This issue will only be approachable when we can generate mutants that are defective for AFRP protease or the AFRP exporter.

Detection of AFRP

Our ability to detect AFRP has always been somewhat variable. There are two factors that might contribute to this variability. First, the particular antiserum preparation used for the immunoprecipitations appears to be critical; antiserum from later bleedings appear to recognize AFRP better than antiserum from the earlier bleedings. No obvious difference has been observed for the recognition of other **a**-factor species. Second, the separation of M and AFRP is extremely sensitive to subtle alterations in electrophoresis conditions; often several independent gel runs are required to achieve sufficient resolution of **a**-factor and AFRP.

Another issue that complicated our analysis is that AFRP, although it can be immunoprecipitated efficiently from the intracellular fraction, is not efficiently immunoprecipitated from the extracellular fraction (unless **a**-factor is absent). One possible explanation for this phenomenon is that the extra 16 Da on AFRP, presumably representing oxidation, may partially obscure the epitope recognized by our antiserum. It is possible that this modification may occur only after AFRP is secreted, which could account for the distinctly different immunoprecipitability of the differently located AFRP molecules. A second possibility we have considered is somewhat more complex, but intriguing. It is based on the analysis of the intracellular fraction of cells expressing fusion constructs; we have observed that we can use **a**-factor antibodies to immunoprecipitate intracellular AFRP-sized molecules that contain foreign residues in place of the normal **a**-factor residues (Chen, 1993). Presumably these species are precipitated indirectly, by virtue of their noncovalent and SDS-resistant association with precursors containing **a**-factor sequences. Therefore, it is possible that intracellular AFRP is also associated with such an SDS-resistant complex in the cell. Were such a structure to exist only inside of cells, then extracellular AFRP would have no way to be efficiently pulled down by our antiserum. More experiments are needed to clarify this potentially interesting point.

It is remarkable that the **a**-factor precursor, which is one of the smallest known peptides in the cell, has so much cellular machinery dedicated to its modification, processing, and export. With the analysis of AFRP described herein, we provide further evidence that the biogenesis of the **a**-factor mating pheromone is even more complicated, but certainly more interesting, than we originally thought because the precursor participates in not one but two maturation pathways each with distinctive proteolytic and export machinery.

ACKNOWLEDGMENTS

We thank S.K. Sapperstein for helpful discussions in the early stages of this study. We also thank Walter K. Schmidt and S.K. Sapperstein for helpful comments on the manuscript. This work was supported by a grant (GM-41223) from the National Institutes of Health to S.M. Mass spectra were obtained at the Middle Atlantic Mass Spectrometry Laboratory, a National Science Foundation-supported Regional Instrumentation Facility.

REFERENCES

Adames, N., Blundell, K., Ashby, M.N., and Boone, C. (1995). Role of yeast insulin-degrading enzyme homologs in propheromone processing and bud site selection. Science *270*, 464–467.

Anderegg, R.J., Betz, R., Carr, S.A., Crabb, J.W., and Duntze, W. (1988). Structure of *Saccharomyces cerevisiae* mating hormone **a**-factor. Identification of *S*-farnesyl cysteine as a structural component. J. Biol. Chem. *263*, 18236–18240.

Ashby, M.N., King, D.S., and Rine, J. (1992). Endoproteolytic processing of a farnesylated peptide in vitro. Proc. Natl. Acad. Sci. USA *89*, 4613–4617.

Berkower, C., and Michaelis, S. (1993). Effects of nucleotide binding fold mutations on STE6, a yeast ABC protein. Molecular Biology and Function of Carrier Proteins, New York: The Rockefeller University Press, 129–146.

Betz, R., Crabb, J.W., Meyer, H.E., Witting, R., and Duntze, W. (1987). Amino acid sequences of **a**-factor mating peptides from *Saccharomyces cerevisiae*. J. Biol. Chem. *262*, 546–548.

Boyartchuk, V., Ashby, M., and Rine, J. (1997). Modulation of Ras and a-factor function by carboxyl-terminal proteolysis. Science *275*, 1796–1800.

Brake, A.J., Brenner, C., Najarian, R., Laybourn, P., and Merryweather, J. (1985). Structure of genes encoding precursors of the yeast peptide mating pheromone a-factor. In: Protein Transport and Secretion, ed. M. J. Gething, Cold Spring Harbor, NY: Cold Spring Harbor Laboratory Press, 103–108.

Brizzio, V., Gammie, A.E., Nijbroek, G., Michaelis, S., and Rose, M.D. (1996). Cell fusion during yeast mating requires high levels of a-factor mating pheromone. J. Cell Biol. *135*, 1727–1739.

Caldwell, G.A., Wang, S.-H., Xue, C.-B., Jiang, Y., Lu, H.-F., Naider, F., and Becker, J.M. (1994). Molecular determinants of bioactivity of the *Saccharomyces cerevisiae* lipopeptide mating pheromone. J. Biol. Chem. *269*, 19817–19826.

Chen, P. (1993). Biogeneis of yeast mating pheromone a-factor. Ph.D. thesis. Baltimore, MD: The Johns Hopkins University School of Medicine.

Chen, P., Sapperstein, S.K., Choi, J., and Michaelis, S. (1997). Biogenesis of the *Saccharomyces cerevisiae* mating pheromone a-factor. J. Cell Biol. *136*, 251–269.

Clarke, S. (1992). Protein isoprenylation and methylation at carboxyl-terminal cysteine residues. Annu. Rev. Biochem. *61*, 355–386.

Cleves, A.E., Cooper, D.N.W., Barondes, S.H., and Kelly, R.B. (1996). A new pathway for protein export in *Saccharomyces cerevisiae*. J. Cell Biol. *133*, 1017–1026.

Field, J., Nikawa, J., Broek, D., MacDonald, B., Rodgers, L., Wilson, I.A., Lerner, R.A., and Wigler, M. (1988). Purification of a RAS-responsive adenylyl cyclase complex from *Saccharomyces cerevisiae* by use of an epitope addition method. Mol. Cell. Biol. *8*, 2159–2165.

Fujimura-Kamada, K., Nouvet, F., and Michaelis, S. (1997). A novel membrane-associated metalloprotease, Ste24p, is required for the first step of NM_2-terminal processing of the yeast a-factor precursor. J. Cell Biol. *136*, 271–285.

Gottesman, M.M., and Pastan, I. (1993). Biochemistry of multidrug resistance mediated by the multidrug transporter. Annu. Rev. Biochem. *62*, 385–427.

He, B., Chen, P., Chen, S.Y., Vancura, K.L., Michaelis, S., and Powers, S. (1991). *RAM2*, an essential gene of yeast, and *RAM1* encode the two polypeptide components of the farnesyltransferase that prenylates a-factor and Ras proteins. Proc. Natl. Acad. Sci. USA *88*, 11373–11377.

Hennekes, H., and Nigg, E.A. (1994). The role of isoprenylation in membrane attachment of nuclear lamins. A single point mutation prevents proteolytic cleavage of the lamin A precursor and confers membrane binding properties. J. Cell Sci. *107*, 1019–1029.

Hochstrasser, M. (1995). Ubiquitin, proteosomes, and the regulation of intracellular protein degradation. Curr. Opin. Cell Biol. *7*, 215–223.

Hochstrasser, M., Ellison, M.J., Chau, V., and Varshavsky. (1991). The short-lived MATα2 transcriptional regulator is ubiquitinated in vivo. Proc. Natl. Acad. Sci. USA *88*, 4606–4610.

Hrycyna, C.A., and Clarke, S. (1992). Maturation of isoprenylated proteins in *Saccharomyces cerevisiae*. Multiple activities catalyze the cleavage of the three carboxyl-terminal amino acids from farnesylated substrates in vitro. J. Biol. Chem. *267*, 10457–10464.

Hrycyna, C.A., Sapperstein, S.K., Clarke, S., and Michaelis, S. (1991). The *Saccharomyces cerevisiae STE14* gene encodes a methyltransferase that mediates C-terminal methylation of a-factor and RAS proteins. EMBO J. *10*, 1699–1709.

Kralli, A., Bohen, S.P., and Yamamoto, K.R. (1995). LEM1, an ATP-binding-cassette transporter, selectively modulates the biological potency of steroid hormones. Proc. Natl. Acad. Sci. USA *92*, 4701–4705.

Kuchler, K., Sterne, R.E., and Thorner, J. (1989). *Saccharomyces cerevisiae STE6* gene product: a novel pathway for protein export in eukaryotic cells. EMBO J. *8*, 3973–3984.

Kunkel, T.A., Roberts, J.D., and Zakour, R.A. (1987). Rapid and efficient site-specific mutagenesis without phenotypic selection. Methods Enzymol. *154*, 367–382.

Macfarlane, R.D. (1981). ^{252}Californium plasma desorption mass spectrometry. Biomed. Mass Spectrom. *8*, 449–453.

Machamer, C.E., and Rose, J.K. (1987). A specific transmembrane domain of a coronavirus E1 glycoprotein is required for its retention in the Golgi region. J. Cell Biol. *105*, 1205–1214.

Michaelis, S. (1993). STE6, the yeast a-factor transporter. Semin. Cell Biol. *4*, 17–27.

Michaelis, S., and Berkower, C. (1995). Sequence Comparison of Yeast ATP-Binding Cassette Proteins, Cold Spring Harbor, NY: Cold Spring Harbor Laboratory Press.

Michaelis, S., and Herskowitz, I. (1988). The a-factor pheromone of *Saccharomyces cerevisiae* is essential for mating. Mol. Cell. Biol. *8*, 1309–1318.

Nijbroek, G.L., and Michaelis, S. (1997). Functional assays for the analysis of yeast *ste6* mutants. Methods Enzymol. (*in press*).

Novick, P., Ferro, S., and Schekman, R. (1981). Order of events in the yeast secretory pathway. Cell *25*, 461–469.

Parham, P. (1992). Antigen presentation. Flying the first class flag [news; comment]. Nature *357*, 193–194.

Powers, S., Michaelis, S., Broek, D., Santa, A.S., Field, J., Herskowitz, I., and Wigler, M. (1986). RAM, a gene of yeast required for a functional modification of RAS proteins and for production of mating pheromone a-factor. Cell *47*, 413–422.

Pryer, N.K., Wuestehube, L.J., and Schekman, R. (1992). Vesicle-mediated protein sorting. Annu. Rev. Biochem. *61*, 471–516.

Resnick, N., and Zasloff, M. (1992). Novel proteases with unusual specificities. Curr. Opin. Cell Biol. *4*, 1032–1036.

Sapperstein, S., Berkower, C., and Michaelis, S. (1994). Nucleotide sequence of the yeast *STE14* gene, which encodes farnesylcysteine carboxyl methyltransferase, and demonstration of its essential role in a-factor export. Mol. Cell. Biol. *14*, 1438–1449.

Schekman, R. (1985). Protein localization and membrane traffic in yeast. Annu. Rev. Cell Biol. *1*, 115–143.

Sikorski, R.S., and Hieter, P. (1989). A system of shuttle vectors and yeast host strains designed for efficient manipulation of DNA in *Saccharomyces cerevisiae*. Genetics *122*, 19–27.

Sisodia, S. (1992). β-Amyloid precursor protein cleavage by a membrane-bound protease. Proc. Natl. Acad. Sci. USA *89*, 6075–6079.

Strazdis, J.R., and MacKay, V.L. (1982). Reproducible and rapid methods for the isolation and assay of a-factor, a yeast mating hormone. J. Bacteriol. *151*, 1153–1161.

Taglicht, D., and Michaelis, S. (1997). A complete catalogue of *Saccharomyces cerevisiae* ABC proteins and their relevance to human health and disease. Methods Enzymol. (*in press*).

Weber, K., Plessmann, U., and Traub, P. (1989). Maturation of nuclear lamin A involves a specific carboxy-terminal trimming, which removes the polyisoprenylation site from the precursor; implications for the structure of the nuclear lamina. FEBS Lett. *257*, 411–414.

Zhang, F.L., and Casey, P.J. (1996). Protein prenylation: molecular mechanisms and functional consequences. Annu. Rev. Biochem. *65*, 241–269.